KEY ROLE OF LYS63-LINKED POLYUBIQUITINATION

IN VIRAL ACTIVATION OF IRF3

APPROVED BY SUPERVISORY COMMITTEE

Dr. Zhijian “James” Chen

Dr. Melanie H. Cobb

Dr. David J. Mangelsdorf

Dr. Yi Liu (Chair)

DEDICATION

This work is dedicated to my husband Jing Yang, for his love and support

KEY ROLE OF LYS63-LINKED POLYUBIQUITINATION IN VIRAL ACTIVATION OF IRF3

by

WENWEN ZENG

DISSERTATION THESIS

Presented to the Faculty of the Graduate School of Biomedical Sciences

The University of Texas Southwestern Medical Center at Dallas

In Partial Fulfillment of the Requirements

For the Degree of

DOCTOR OF PHILOSOPHY

The University of Texas Southwestern Medical Center at Dallas

Dallas, Texas

March, 2009

KEY ROLE OF LYS63-LINKED POLYUBIQUITINATION

IN VIRAL ACTIVATION OF IRF3

WENWEN ZENG, Ph.D.

The University of Texas Southwestern Medical Center at Dallas, 2009

Mentor: ZHIJIAN "JAMES" CHEN, Ph.D.

Viral nucleic acids exposed during invasion and proliferation are detected by mammalian cells through receptors belonging to pattern-recognition receptors family (PRRs). Among PRRs, RIG-I-like receptors (RLRs), including RIG-I, MDA5 and LGP2, are responsible for sensing intracellular viral RNAs. MAVS, a mitochondria-localized transmembrane protein, transduces signaling from RIG-I and MDA5 to activate downstream transcription factors IRF3 and NF-κB, which contribute to the induction of IFNβ. Despite growing list of components revealed in RIG-I/MAVS/IRF3 pathway,

molecular mechanism by which MAVS activates IRF3 upon viral infection has remained largely unclear. In current study, employing a cell-free system together with conventional fractionation procedures, Ubc5 was identified as a specific ubiquitin-conjugating enzyme (E2) involved in IRF3 activation. Taking advantages of inducible-RNAi strategy, catalytically active Ubc5 was shown to be essential for viral activation of IRF3. Furthermore, evidences were obtained indicating that Lys63-linked polyubiquitination played a key role in MAVS-mediated IRF3 activation both *in vitro* and *in vivo*. Finally, NEMO was demonstrated to function as a ubiquitin-chain adaptor recruiting and activating TBK1, the kinase for IRF3 phosphorylation. Those results offered insights into the mechanism underlying IRF3 activation mediated by K63-linked polyubiquitination.

TABLE OF CONTENTS

PRIOR PUBLICATION

1. **Zeng, W.**, and Chen, Z.J.: MITAgating viral infection. ***Immunity***, 29: 513-515, 2008.

LIST OF FIGURES

CHAPTER I: INTRODUCTION

Immunity is elaborately developed in the metazoans, which helps the organisms defending various pathogenic challenges encountered during the lifetime. In vertebrates, it has further evolved into two conceptually distinct yet tightly intertwined systems, innate and adaptive immunities, which together combat invading pathogens with greatly enhanced efficiency. Generally, most pathogens are detected and resolved by innate immune responses within hours, whereas second-phase response is taken over by adaptive immunity that could last for days or even years. As the frontier to keep the invaders in check, critical functions of innate immunity have been extensively explored in the past two decades. Moreover, key roles of innate immunity have been emphasized for appropriate mobilization of adaptive immune response (Clark and Kupper, 2005).

Innate Immune System

As a model for primary innate immunity in the metazoans, fruit fly *Drosophila melanogaster* has been widely studied in the field. Innate immune system in fly consists of three parts, i.e., humoral response, cellular response and

melanization. Humoral response is elicited by Toll or Imd pathways, which are major sensing mechanisms for fungal or bacterial infection in Drosophila. Upon activation, the fat body representing an analog of mammalian liver secretes several families of anti-microbial peptides. Open circulatory blood system then rapidly disperses those anti-microbial peptides to directly target and destroy invading microbes. In a separate cellular response, blood cells in fly can clear pathogens through phagocytosis, resembling a function of neutrophil or macrophage in mammals (Ferrandon et al., 2007; Stuart and Ezekowitz, 2008). Finally, as a unique immune response in the phylum *Arthropoda*, production and deposition of melanin pigments on pathogens work in concert with the other two systems to eliminate invading pathogens (Williams, 2007).

Similar to invertebrates, innate immunity in mammals is composed of a variety of soluble factors and cell types, although in a more sophisticated network. Particularly, besides physically preventing pathogenic invasion, epithelium lining at interface between environment and inner body functions as a critical immunologic barrier. Infection of epithelial cells, fibroblasts or dendritic cells can induce a rapid production of cytokines, chemokines and other co-stimulatory molecules, which cause inflammation, anti-microbial scavenging and attraction of

phagocytes. Moreover, cytokines also alert to the host body of pathogenic presence to boost adaptive immune response. As another important part of innate immunity, complement system composing of multiple plasma proteins binds foreign pathogens either to trigger cytolysis or to opsonize their removal by phagocytotic cells (Palm and Medzhitov, 2009; Underhill and Ozinsky, 2002).

Receptors for Pathogen-Associated Molecular Patterns

To elicit effective innate immunity, a set of germline-encoded receptors, namely Pathogen Recognition Receptors (PRRs), are key cellular sensors to detect various microbial or viral components called Pathogen-Associated Molecular Patterns (PAMPs). Several characterized PAMPs include lipopolysaccharide (LPS) from Gram-negative bacteria, lipotechoic acids from the Gram-positive bacteria, flagellin from bacteria, double-stranded RNA (dsRNA) or single-stranded RNA (ssRNA) from viruses, unmethylated CpG DNA from bacteria or viruses, and glucans from fungus (Fig. 1). Generally, PRRs distinguish PAMPs from self-components according to repeating structural elements unique to particular pathogens. Taking advantages of the fact that PAMPs always represent essential building blocks for pathogen survival and also remain largely

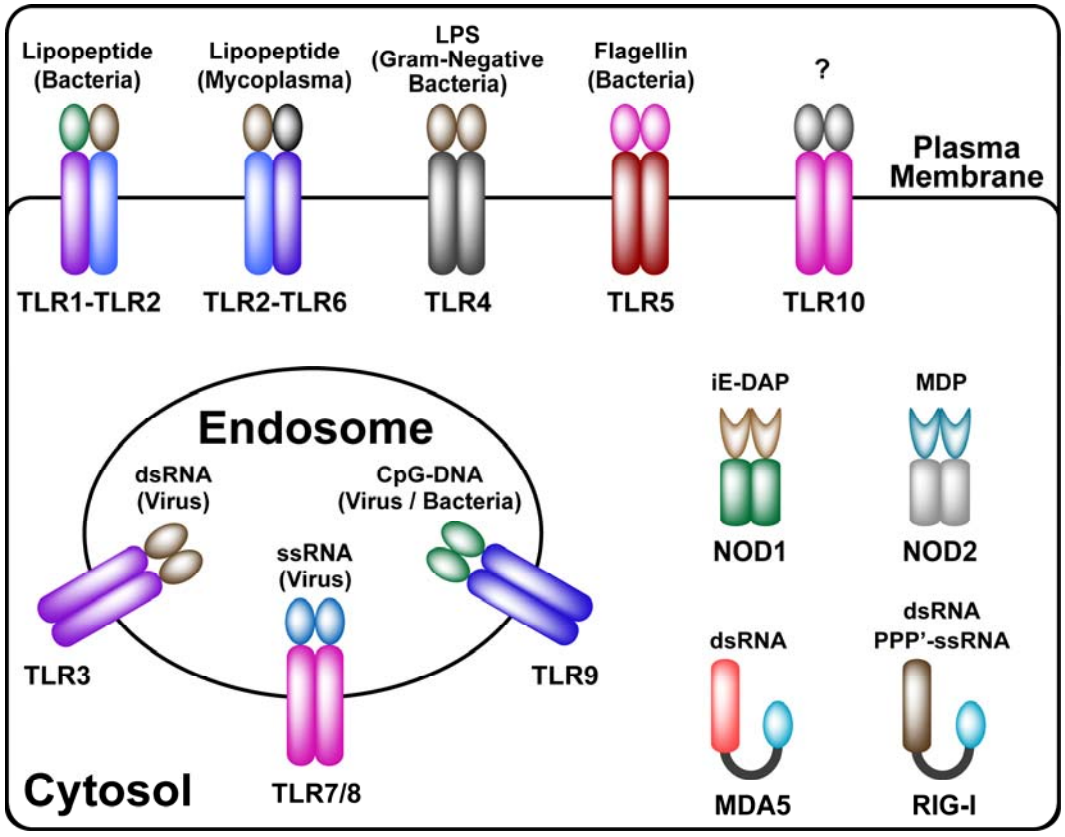

Figure 1. Pathogen Recognition Receptors in Human Cells

Residing on plasma membranes or endosomal membranes, Toll-like receptors (TLRs) function as homo- or hetero-dimer in recognition of indicated pathogen-associated molecular patterns (PAMPs) from bacteria or viruses. In cytosol, NOD-like receptors and RIG-I-like receptors sense the presence of indicated PAMPs. For illustrative purpose, NOD1 and NOD2 are chosen as representatives of NOD-like receptor family. See text for detailed description.

unchanged across species, evolvement of PRRs has efficiently covered a broad spectrum of pathogens (Janeway and Medzhitov, 2002).

Originally identified through map-based cloning of mouse genetics, Toll-like receptors (TLRs) have been the first documented members of PRRs (Poltorak et

al., 1998). TLRs are conserved from insects to mammals, and widely expressed in various cells types, including epithelial cells, fibroblasts, antigen-presenting macrophages and dendritic cells, and certain types of B and T lymphocytes. In human genome, 10 members of TLRs have been characterized (Kawai and Akira, 2008). All of TLRs belong to class -I transmembrane protein, with a leucine-rich ligand-binding domain facing to extracellular or luminal compartments, and a Toll/interleukin-1 (IL-1) receptor (TIR) domain for transducing signal on cytoplasmic side (O'Neill and Bowie, 2007). Interestingly, several recent studies have shown that ectodomain of TLR9 requires a proteolytic cleavage to generate functional receptor (Park et al., 2008).

Localized on either cell surface or endosomal membranes, TLRs recognize one or more classes of PAMPs as homo-dimer or hetero-dimer (Fig. 1). For instance, TLR1, TLR2, and TLR6 on plasma membrane bind lipopeptides from fungi, bacteria or protozoa. And TLR4 recognizes LPS exposed to cell surface by Gram-negative bacteria. On the other hand, TLR3, TLR7, TLR8 and TLR9 sense nucleic acids derived from proliferating pathogens in endosomal compartments to initiate signaling (Beutler et al., 2006). Given the localization and topology of TLRs, it is of note that they are not accessible to pathogens already invading

inside cells. Therefore, involvement of other mechanisms to detect intracellular pathogens should be equally critical to a success of innate immune system.

In the past decade, researchers have unveiled two other groups of PRRs, namely nucleotide-binding oligomerization domain (NOD)-like receptors (NLRs) and RIG-I like receptors (RLRs) (Fig. 1). In human genome, NLR family is predicted to contain more than 20 members. Several NLRs have been demonstrated in detecting intracellular bacterial components. For instance, as two of the best studied NLRs, NOD1 and NOD2 are proposed to recognize γ-D-glutamyl-meso- diaminopimelic acid (iE-DAP) and muramyl dipeptide (MDP) from bacterial cell wall, respectively (Fig. 2) (Fritz et al., 2006).

For RLR family, current knowledge has suggested them as main sensors for viral nucleic acids, which are inevitably generated during invasion and amplification of viral genomes in cytosol (Takeuchi and Akira, 2008). 3 members of RLR family exist in mammalian genomes, i.e., retinoic acid-inducible gene I (RIG-I), melanoma differentiation-associated gene 5 (MDA5), and laboratory of genetics and physiology 2 (LGP2). By recognizing structurally distinct nucleic acids, RLRs offer a broad coverage for viral RNA species (Fig. 1). Taken together, evidences have indicated that PRRs for detection of intracellular presence of

PAMPs not only alert a dangerous ongoing invasion, but also represent one more layer of guard functioning complementarily with TLRs (Meylan et al., 2006).

Viral Sensing Pathways

Among highly infectious pathogens are a large number of viruses. Viral infections often result in common but severe pathologies in humans, e.g., influenza A virus, hepatitis C virus (HCV), and human immunodeficiency virus (HIV). Evolutionarily, viruses have developed complex relationships with host organisms, and usually depend on host cellular machineries to synthesize essential components for their proliferation, including nucleic acids and envelop proteins.

To counter-strike viral infection, innate immunity has evolved multiple strategies to sense viral nucleic acids to elicit efficient anti-viral responses. Firstly, TLR3, TLR7, TLR8 and TLR9 are specialized in viral nucleic acids recognition. Within endosomal compartments, unmethylated CpG-containing viral DNAs are recognized by TLR9, whereas viral ssRNAs and dsRNAs activate TLR7/8 and TLR3, respectively (Beutler et al., 2007). Structural study has revealed that ligand-binding facilitates rearrangement and dimerization of the receptors, which further triggers the recruitment of downstream TIR domain containing adaptor

proteins such as myeloid differentiation factor 88 (MyD88) by TLR7/8 and TLR9, or TIR-domain-containing adaptor protein inducing IFNβ (TRIF) by TLR3 (Fig. 2) (Choe et al., 2005; Jin and Lee, 2008).

Existence of TLR-independent receptor(s) for viral RNAs had been suggested based on evidences that TLR3-deficient cells could still respond to stimulation by poly-inosinic acid-cytidylic acid (polyI:C), a synthetic analog of viral dsRNA (Alexopoulou et al., 2001). Such putative receptors were later identified as RLRs, including MDA5 and RIG-I (Kang et al., 2002; Yoneyama et al., 2004). Research with gene-targeted deletion has shown that MDA5 and RIG-I differentially respond to distinct viruses. For instance, MDA5 is required for effective response against picornaviruses such as encephalomyocarditis virus (EMCV) and Theiler's virus, whereas RIG-I is essential in response to a variety of viruses including Japanese encephaloitis virus, HCV, vesicular stomatitis virus (VSV), Sendai virus (SeV) and influenza A virus (Gitlin et al., 2006; Kato et al., 2006; Takeuchi and Akira, 2008). Moreover, the two receptors also function cooperatively in response to West Nile virus (Fredericksen et al., 2008).

Different involvement of RIG-I and/or MDA5 in recognition of various viruses can be partially explained by their specificity to structurally distinct RNA

species derived from viruses. RIG-I and MDA5 preferentially recognize short and long viral dsRNAs, respectively. 5'-triphosphate ssRNAs from viral genome or transcribed during viral proliferation is specifically recognized by RIG-I (Hornung et al., 2006; Kato et al., 2008; Pichlmair et al., 2006).

In contrast to well-characterized roles of RIG-I and MDA5, function of LGP2 is more complicated. Studies have proposed that LGP2 may act as a dominant-negative regulator of RIG-I and MDA5 by competitively binding to viral RNAs (Rothenfusser et al., 2005; Yoneyama et al., 2005). However, LGP2-deficient mice show elevated production of interferons in response to VSV, but paradoxically impaired interferons induction by EMCV infection (Venkataraman et al., 2007). Given the fact that viral RNAs of VSV are mainly detected by RIG-I and those of EMCV by MDA5, it remains possible that LGP2 may regulate RIG-I and MDA5 pathways through different mechanisms (Pippig et al., 2009). Since LGP2 does not contain CARD-domain like the other two RLRs, it is still an open question of whether LGP2 can directly transduce downstream signaling through MAVS (see below).

Molecular Pathway of Intracellular Viral RNA Recognition

Engagements of TLRs or RLRs result in activation of transcription factors including IRF3 and NF-κB, which converge on promoter region of IFNβ to form a complex called enhanceosome in activating gene transcription (Fig. 2) (Panne, 2008). In this study, intracellular viral RNA recognition was investigated to elucidate the molecular mechanism for activation of downstream transcription factors, especially IRF3.

RIG-I is composed of two tandem CARD domains on the N-terminus followed by a DexD/H-Box helicase domain, and a C-terminal repressor domain (Cui et al., 2008; Yoneyama et al., 2005). DexD/H helicases form a large protein family, which are proposed to unwind RNA molecules in ATP/GTP-dependant manner (Tanner and Linder, 2001). Several structural and biochemical analyses have suggested that activation of RIG-I by viral RNAs is likely to be mediated by two physically separated but functionally intertwined events. Firstly, mutations of ATP-binding site on DexD/H helicase domain resulted in loss-of-function of RIG-I, indicating that RNA helicase activity is indeed required for protein activation. Secondly, RIG-I remains suppressed in non-infected cells due to auto-inhibition of intra-molecular interaction between CARD domains and C-terminal repressor domain. Upon binding of viral RNAs, N-terminal CARD

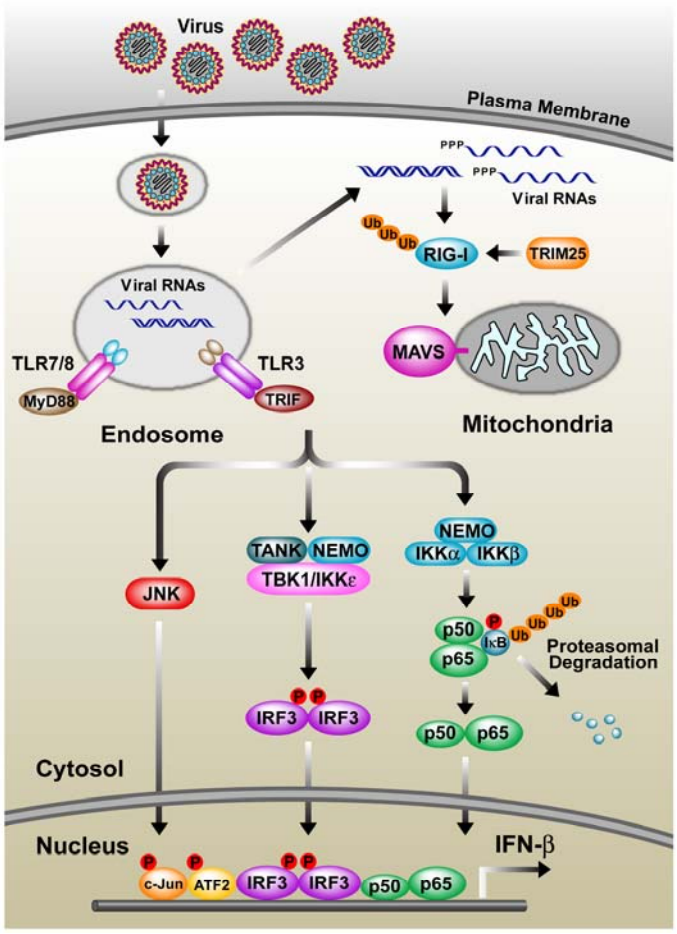

Figure 2. Viral Induction of Interferon-β Production
Upon infection, the presence of viral RNAs in endosomal luminal compartment activates TLR7/TLR8 or TLR3, which recruits adaptors MyD88 or TRIF, respectively. During viral proliferation, the appearance of viral RNAs in cytosol is recognized by RIG-I, which is ubiquitinated by TRIM25 to further transduce signal to mitochondria localized adaptor MAVS. TLR3 and RIG-I pathways share the three major downstream signaling cascades, leading to activation of transcription factors c-Jun/ATF2, IRF3, and NF-κB, together of which form the enhanceosome on the promoter of interferon-β to activate gene transcription. See text for detailed description.

domains of RIG-I may get exposed and oligomerized, which is believed to achieve an active form (Cui et al., 2008). In support of the notion, overexpression of truncated RIG-I composing of only N-terminal CARD domains could efficiently activate the downstream signals in the absence of viral infection (Yoneyama et al., 2004).

The fact that overexpression of RIG-I CARD domains was sufficient to induce interferon production has suggested that a downstream adaptor possibly associates with activated RIG-I through CARD-CARD domain interaction. In fact, CARD domains are widely involved in inter-molecular interactions, e.g., several components involved in apoptosis are signaling through direct interaction between CARD domains (Martinon and Tschopp, 2004). Indeed, bioinformatic search for CARD domains homologous to RIG-I led to identification of mitochondrial antiviral signaling protein (MAVS; also known as VISA, CARDIF, IPS-1), which possesses two CARD domains on its N-terminus (Kawai et al., 2005; Meylan et al., 2005; Seth et al., 2005; Xu et al., 2005). As predicted, interaction between RIG-I and MAVS is mediated by homotypic CARD domains. Unexpectedly, MAVS contains a single transmembrane domain at its C-terminus, anchoring the protein to outer membrane of mitochondria (Seth et al., 2005). More importantly, mitochondrial targeting is critical for MAVS signaling, since mutant versions of the protein without transmembrane or with transmembrane targeting endoplasmic-reticulum were devoid of normal function (Seth et al., 2005). Although several hypotheses have been proposed for the intriguing localization of MAVS, a definitive explanation on molecular or evolutionary level

is still missing (Baril et al., 2009; Tang and Wang, 2009).

In MAVS-deficient mice, multiple cells types including conventional dendritic cells (cDC), macrophages and epithelial cells showed defective interferon production in response to SeV and VSV, suggesting that MAVS is functioning downstream of RIG-I (Kumar et al., 2006; Sun et al., 2006). However, infection of MAVS-deficient mice with VSV resulted in a normal level of plasma interferons comparing to wild-type littermates, probably reflecting the fact that plasmacytoid dendritic cells (pDC) could utilize MAVS-independent TLR pathways in response to viral RNAs (Sun et al., 2006). But adding to the complexity, MAVS-deficient mice still demonstrated higher mortality rate due to increased viral load (Kumar et al., 2006; Sun et al., 2006). This observation may emphasize the idea that not only systemic but also local production of interferons from infected tissues is important for successful anti-viral immunity in mammals.

Signaling from MAVS leads to activation of multiple kinases, including IKK complex (IKKα/IKKβ/NEMO), TBK1 (or IKKε), and JNK (Fig. 2). IKK complex phosphorylates the inhibitory IκB proteins, resulting in their ubiquitination and subsequently degradation by proteasomal pathway, which releases NF-κB to enter into nucleus.

In a separate branch, TBK1 functions as a kinase to activate IRF3. IRF3 undergoes dimerization upon its phosphorylation, and the dimer translocates into nucleus (Fitzgerald et al., 2003; Sharma et al., 2003). Besides TBK1, IKKε is another kinase mediating IRF3 activation, which shares about 60% homology to TBK1. TBK1 and IKKε exhibit different patterns of tissue distribution, i.e.., TBK1 is ubiquitously expressed, while IKKε is restricted to certain cell types such as macrophages in mouse (Perry et al., 2004). Moreover, expression level of IKKε could be induced by viral infection (Lin et al., 2006). Such differences in expression pattern could explain that TBK1-deficient MEF cells showed dramatic decrease of viral induction of interferons, whereas no obvious defect was observed in IKKε-deficient macrophages (McWhirter et al., 2004).

Despite extensive studies, mechanism underlying downstream events of MAVS-mediated TBK1/IKKε activation has remained largely unclear. Various proteins have been reported to be involved in this process, e.g., NEMO (Zhao et al., 2007), TRADD (Michallet et al., 2008), STING (also known as MITA) (Ishikawa and Barber, 2008; Zhong et al., 2008), TANK (Guo and Cheng, 2007), NAP1 (Sasai et al., 2006), and SINTBAND (Ryzhakov and Randow, 2007). Among those components, NEMO-deficiency in MEF cells completely blocked

interferons production and renders cells highly susceptible to viral infection (Zhao et al., 2007). TRADD-deficient MEF cells showed a partial decrease of IFNβ production when infected with SeV and VSV (Michallet et al., 2008). STING-deficiency resulted in no defect of IFNβ production in dendritic cells or macrophages, but decreased IFNβ production in MEF cells, which might reflect the existence of redundant factors in particular cell types (Ishikawa and Barber, 2008). Furthermore, RNAi-knockdown of TANK, NAP1, or SINTBAD all produced a partial defect in IFNβ production upon viral infection. Together with biochemical studies showing that TANK (also NAP1 and SINTBAD) could mediate interaction between TBK1 and NEMO (Chariot et al., 2002), it has become possible that TANK, NAP1 and SINTBAD might function redundantly as a bridge between NEMO and TBK1 to form a complex for phosphorylation and activation of IRF3. However, how viral-activated MAVS transduces signal to TBK1 remains unexplored.

Anti-Viral Effect of Interferons

As a hallmark of mobilization of innate immunity against viral infection, activation of TLRs or RLRs leads to the production of interferons. Interferons are

widely involved in innate and also adaptive immunity, and mainly consist of type-I and type-II classes. Type-I interferons include multiple subtypes of IFNα and a single IFNβ, and type-II interferon contains only IFNγ. Among numerous functions of type-I interferons, the most crucial function of type-I interferons is in anti-viral response, which was firstly described in 1950s when researchers found a substance from influzenza virus-infected tissues could render resistance to further viral infection (Isaacs and Lindenmann, 1957; Isaacs et al., 1957).

Functions of type-I interferons are mediated by a cell surface receptor composed a hetero-dimer of IFNAR1 and IFNAR2. Binding of IFNα or IFNβ to the receptor results in recruitment and activation of two downstream kinases, Tyk2 and Jak1. Tyk2 and Jak1 then phosphorylate STAT1 and STAT2, which hetero-dimerize and further associate with interferon regulatory factor 9 (IRF9). STAT1/STAT2/IRF9 complex translocates into nucleus to activate transcription of hundreds of interferon-stimulated genes (ISGs), which are directly or indirectly involved in anti-viral responses (Vilcek, 2006). For instance, PKR is one of the well-studied ISGs, which is activated by dsRNA and phosphorylate eIF2α, leading to a blockage of global translation of most cellular and viral mRNAs (Williams, 2001).

In addition to local suppression of viral proliferation, type-I interferons also facilitate adaptive immunity. For instance, type-I interferons are known as major regulators for dendritic cells, which drive maturation of dendritic cells and also enhance viral-antigen cross-presentation through induced expression of major histocompatibility complex class I (MHC-I). Furthermore, IFNα and IFNβ could support the survival and proliferation of activated T cells as well as mature B cells, sustaining adaptive immune response to battle viral challenges. Finally, interferons can activate cytotoxic cells such as natural killer cells in direct elimination of infected cells. As an emphasis on the indispensable roles of interferons in host defense against viruses, gene-targeted deletion of interferon-receptor rendered mice extremely susceptible to various viruses (Le Bon and Tough, 2002; Stetson and Medzhitov, 2006).

Viral Evasion from Innate Immunity

To ensure successful infection and transmission, viruses have evolved multiple ways to evade or even hijack anti-viral pathways in mammals. Particularly, suppressing production of type-I interferons has been one of the commonly employed strategies. Suppression of interferons signaling not only

acutely blocks innate immune response, but also effectively inhibits activation of adaptive immunity, resulting in a failure to clear viral-infected cells and chronic infections (Grandvaux et al., 2002; Katze et al., 2008).

Several examples have been documented regarding the mechanisms of how viruses interfere with TLR and RLR pathways in host cells. For instance, HCV, a single-stranded RNA virus, is well known for its ability to modulate innate immunity. Among viral nonstructural proteins, NS3/4A is a cysteine protease which cleaves the polypeptide encoded by viral mRNA. However, the same protease has been found to cleave both TRIF and MAVS, the two critical adaptor proteins in TLR3 and RIG-I/MDA5 pathways, respectively. Therefore, NS3/4A could simultaneously abolish viral induction of interferons by either TLR or RLR pathways (Bode et al., 2007; Gale and Foy, 2005; Li et al., 2005a; Li et al., 2005b). Another RNA virus, influenza A virus is able to antagonize interferons induction partially through direct binding of viral NS1 protein with RIG-I and therefore block its function (Hale et al., 2008; Mibayashi et al., 2007). As one more example, vaccinia virus, a double-stranded DNA virus, utilizes multiple approaches to evade host immunity. Firstly, virus genome encodes an E3L protein, which binds dsRNA generated during viral proliferation to hide the nucleic acids

from being recognized by RIG-I pathway (Bowie and Unterholzner, 2008; Xiang et al., 2002; Zhang and Samuel, 2008). Secondly, viral A46R protein contains a TIR domain resembling that on TLRs, and can associate with TRIF in a dominant-negative manner (Stack et al., 2005).

Extensive studies on how human bodies respond to viral infection and how different viruses evade immunity with various strategies have offered invaluable insights into the interplay between viruses and host defense. Such valuable knowledge not only significantly advances our understandings of distinct signaling pathways involved in anti-viral response, but also helps to reveal novel approaches for therapeutic prevention or treatment of viral infection in humans. For instance, since NS3/4A protease of HCV is responsible for suppression of innate immunity, inhibition of NS3/4A protease by small-molecule inhibitors, or expression of non-cleavable MAVS has been shown to efficiently restore interferons production (Lamarre et al., 2003; Li et al., 2005b). Similarly, given immunologic-repressive function of NS1 protein, attenuated strains of influenza A virus containing truncated NS1 are under investigations for potential vaccine due to their higher potency to induce interferons and production of neutralizing antibodies in animals and humans (Steel et al., 2009).

Ubiquitination in Signaling Pathway

Ubiquitination is a covalently post-translational modification by attachment of single or multiple ubiquitin, a 76 amino acid globular protein. It is accomplished through three-step reaction cascade catalyzed by ubiquitin-activating enzyme (E1), ubiquitin-conjugating enzyme (E2) and ubiquitin ligase (E3) (Fig. 3A). Human genome contains 2 E1s, approximately 40 E2s, and more than 600 E3s (Chen and Sun, 2009; Pickart, 2001).

For a ubiquitination reaction cycle, ubiquitin is first activated and conjugated to E1 in an ATP-dependent manner, forming a thioester bond between the C-terminal Gly-residue of ubiquitin and active site Cys-residue on E1. Through trans-thiol esterification, ubiquitin is then transferred to various E2s, a protein family all sharing a core domain with a conserved active site Cys-residue. In the next step of ubiquitination reaction, three groups of E3s are defined according to distinct domain structures, i.e., homology to the E6-associated protein carboxyl terminus (HECT) domain, really interesting new gene (RING) domain, and a variant of RING domain called U-box domain. It is generally believed that RING domain and U-box domain E3s function as scaffold to assemble ubiquitin-charged E2s and target proteins for direct transferring of ubiquitin from E2s to targets. In

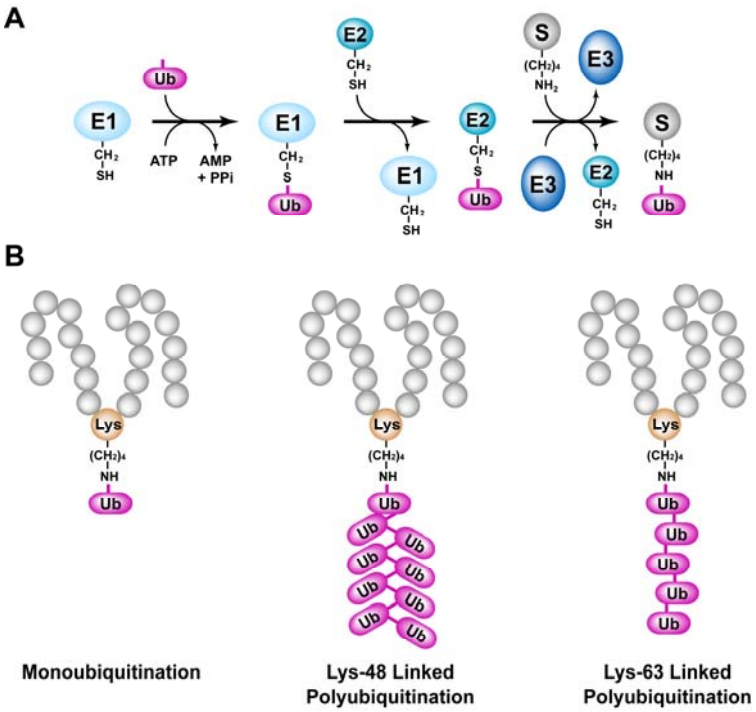

Figure 3. Diagram of Ubiquitination Reaction (A) Reaction cascade of ubiquitination. Ubiquitin is activated by E1 in ATP-dependent manner, and relayed to E2 and E3, resulting in the final attachment to a protein substrate on Lys-residue. (B) Distinct forms of ubiquitination. Modification by ubiquitin with only one round of reaction leads to mono-ubiquitination. Repetitive addition of ubiquitin to substrate results in the formation of ubiquitin-chain, or polyubiquitination. Depending on specific Lys residues within ubiquitin utilized for chain elongation, two common forms of polyubiquitination exist in structurally distinct Lys48- or Lys63-linkage.

contrast, active site Cys-residue of HECT domain E3s can be conjugated with ubiquitin by E2s through trans-thiol esterification, and ubiquitin-charged E3s then attach ubiquitin to target proteins. Therefore, for a particular ubiquitination reaction, specificity could be determined by at least two layers of regulation, i.e., one E2 only interacts with certain E3s, and a limited number of substrates are recognized by one particular E3 (Pickart, 2004; Pickart and Eddins, 2004).

Protein substrates can be conjugated by either mono-ubiquitin or

poly-ubiquitin chain (Fig. 3B). For mono-ubiquitination, the C-terminus of a single ubiquitin is conjugated to ε-NH_2 of Lys-residue of target proteins. But in certain cases, ubiquitin can also be attached to N-terminus of target proteins (Ciechanover and Ben-Saadon, 2004). Mono-ubiquitination has been described in several signaling processes, e.g., serving as recognition signal for transport of membrane-bound receptors to endosomes or lysosomes (Hicke and Dunn, 2003). Other examples include mono-ubiquitination of histones during transcriptional elongation. (Pavri et al., 2006).

Ubiquitin itself contains seven Lys-residues. As a result, in addition of attaching to Lys-residue on target proteins, successive ubiquitin moieties can be conjugated to the former ubiquitin to generate ubiquitin chain. All Lys residues (K6, K11, K27, K29, K33, K48, and K63) of ubiquitin are able to support ubiquitin-chain formation (Peng et al., 2003). Among those different linkages, the first and also best characterized one is K48-linked polyubiquitination, in which ubiquitin-chain is conjugated through Lys48 residue. Numerous studies have demonstrated that, from yeast to humans, K48-linked polyubiquitination serves as a recognition signal for protein degradation by proteasomal pathway.

Since early 1990s, polyubiquitination with K63-linkage has gained increased

attentions due to its ever expanding roles in various singling pathways, e.g., DNA repair, endocytosis, inflammation, and immunological response (Chen and Sun, 2009). It has been accepted that K63-linked ubiquitin-chain could serve as a platform for recruitment of adaptor proteins into close proximity to exert their functions. Furthermore, polyubiquitination with heterogeneous linkages has been observed, at least *in vitro* (Kirkpatrick et al., 2006). But, it is far from clear whether those ubiquitin chains with mixed linkages could exhibit different topology, or serve a role in any biological process in cells.

Very recently, growing evidence has suggested that polyubiquitination might play a critical role in RLR pathway. TRIM25 has been reported as an E3 ubiquitin-ligase mediating K63-polyubiquitination of RIG-I, which modification appears to be essential for RIG-I activation (Gack et al., 2007). Also, deficiency of TRAF3, a member of TRAF E3 family, resulted in a decrease of interferon production in MEF cells (Hacker et al., 2006; Oganesyan et al., 2006; Saha et al., 2006). Furthermore, consistent with a putative role of polyubiquitination in RIG-I/MAVS signaling cascade, two de-ubiquitination enzymes CYLD and DUBA, which are proteases specific for cleavage of iso-peptide bond between ubiquitin moieties, have been identified as negative regulators in viral activation

of IRF3 (Friedman et al., 2008; Kayagaki et al., 2007; Zhang et al., 2008). Taken together, several novel components have been revealed, all of which clearly imply a role of K63-polyubiquitination in RIG-I/MAVS/IRF3 pathway.

Goal of Current Research

Molecular mechanism underlying viral activation of IRF3 will be explored. New insight into RIG-I/MAVS/IRF3 pathway will facilitate an accurate description of viral recognition and innate immunity in human bodies. Moreover, such knowledge will be of great interest to therapeutic intervention, which remains challenging for treatment of fatally infectious diseases, especially those caused by viruses.

CHAPTER II: RESULTS

Establishment of Biochemical Assay for IRF3 Activation

To dissect the biochemical mechanism for MAVS-mediated IRF3 activation, an *in vitro* assay was established by Dr. Lijun "Josh" Sun in the laboratory. In this assay, MAVS present on mitochondria isolated from viral-infected cells demonstrated the ability to activate the downstream component(s) in cytosol, leading to phosphorylation and dimerization of IRF3.

Briefly, mitochondria fraction (P5) and cytosolic fraction (S5 or S100) were prepared through sequential centrifugation of homogenates from the cells mock treated or infected with Sendai Virus (SeV, Fig. 4A). *In vitro* translated ^{35}S-labeled IRF3 was used as a substrate, and its dimerization was visualized by autoradiography following native poly-acrylamide gel electrophoresis (PAGE). Shown in Fig. 4B, inclusion of P5 from viral-infected cells with S100 from uninfected cells in the presence of ATP resulted in a slower migrating ^{35}S-labeled band, corresponding to IRF3 dimer on native PAGE. To confirm that the dimerization of IRF3 was indeed due to its phosphorylation, the same set of reactions in parallel was analyzed by SDS-PAGE. Slower migrating IRF3 band

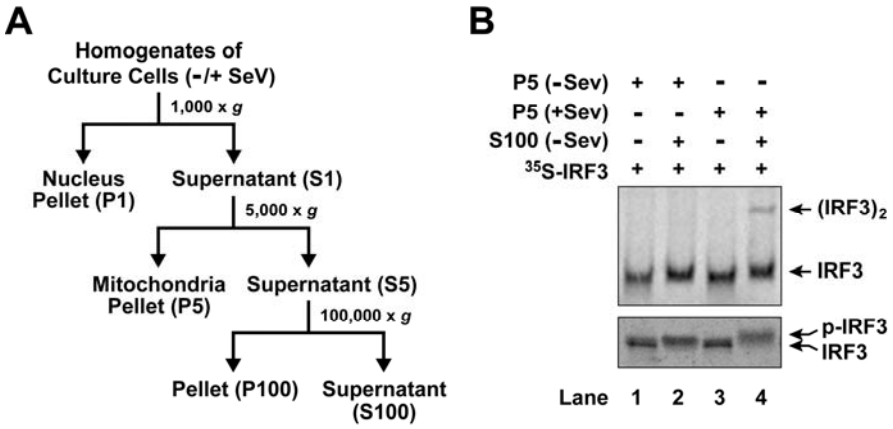

Figure 4. Establishment of Biochemical Assay for IRF3 Activation

(A) Diagram of fractionation procedure of cell homogenates. Culture cells without or with infection by Sendai virus (-/+SeV) was homogenized in hypotonic buffer, followed by sequential centrifugations to prepare mitochondria fraction (P5) and cytosolic supernatants (S5 or S100) as described in **Experimental Procedures**.

(B) Viral activation of IRF3 *in vitro*. Each 10-µl reaction contained 4 µg of indicated P5 from HEK293-MAVS cells without (-SeV) or with (+SeV) viral infection, 30 to 40 µg of S100 from HEK293 cells without viral infection (-SeV), and 0.5 µl of ^{35}S-IRF3 in buffer containing 20 mM HEPES-KOH (pH 7.0), 2 mM ATP and 5 mM $MgCl_2$. After incubation at 30^{o}C for 1 hour, samples were subjected to native PAGE, and dimerization of ^{35}S-IRF3 was visualized by autoradiograph (upper panel) as described in **Experimental Procedures**. Phosphorylation of IRF3 in replicate reactions was determined by SDS-PAGE (lower panel).

indicative of phosphorylated form was apparent only when both of S100 and viral-activated P5 were included (Fig. 4B, lower panel). The reaction was dependent on viral-activated mitochondria (or MAVS), since the formation of IRF3 dimer was not observed with P5 from uninfected cells (Fig. 4B, Lane 1 and 2). In addition, when S100 was omitted, IRF3 dimerization was also abolished (Fig. 4B, Lane 3), indicating soluble component(s) in cytosol was required.

Given the complexity of signaling pathway in IRF3 activation (Fig. 2), it was obligate to investigate the authenticity of the *in vitro* assay. When the assays were carried out with P5 from viral-infected cells depleted of either RIG-I or MAVS by RNAi, the formation of IRF3 dimer was diminished (Fig. 5A and B), consistent with the notion that IRF3 dimerization depends on viral-activated MAVS. When S5 was derived from HEK293 cells depleted of TBK1 by RNAi or NEMO-deficient MEF cells, IRF3 dimerization was also largely blocked (Fig. 5C and Fig. 15C), in accordance with the fact that TBK1 and NEMO both function downstream of MAVS in IRF3 activation. Previous studies reported that overexpression of N-terminal domain of RIG-I (RIG-I-N) or MAVS could potently activate IRF3 (Seth et al., 2005; Yoneyama et al., 2004). Consistently, when P5 was isolated from the cells transiently overexpressing RIG-I-N or MAVS without viral infection, it could efficiently support the formation of IRF3 dimer (Fig. 5D and E). Of note, besides the exogenous substrate of ^{35}S-IRF3, the dimerization of endogenous IRF3 could also be observed (Fig. 5C). Taken together, the biochemical assay faithfully recapitulated the epistatic interactions of several components involved in MAVS-mediated IRF3 activation.

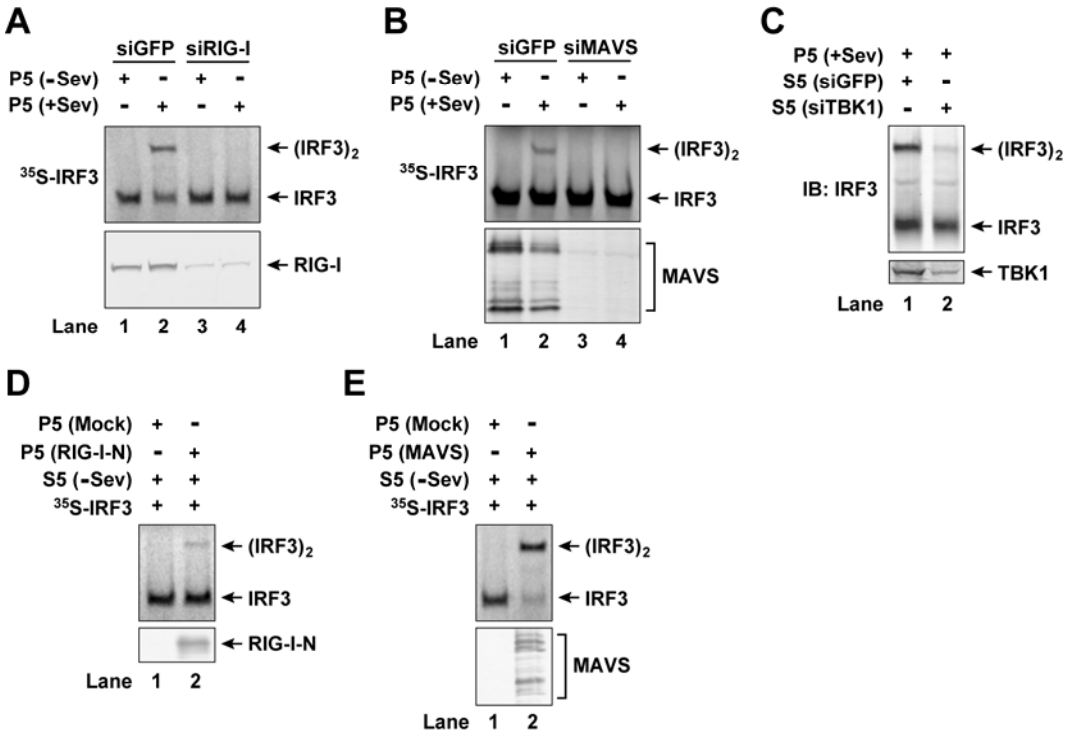

Figure 5. Authenticity of *In Vitro* Assay for IRF3 Activation

Each 10-μl reaction was set up as described in Fig. 4B.

(A) RIG-I functions upstream of MAVS. Reactions contained P5 of HEK293 cells transfected by siRNA against GFP or RIG-I, without or with viral infection, and S5 of HEK293 cells without viral infection. Efficiency of RIG-I-knockdown was determined by immunoblot analysis of S5 fractions (lower panel).

(B) MAVS is required for IRF3 activation. Reactions contained P5 of HEK293 cells transfected by siRNA against GFP or MAVS, without or with viral infection, and S5 of HEK293 cells without viral infection. Efficiency of MAVS-knockdown was determined by immunoblot analysis of P5 fractions (lower panel).

(C) IRF3 activation depends on TBK1. Reactions contained P5 of HEK293 cells with viral infection, and indicated S5 of HEK293 cells transfected by siRNA against GFP or TBK1. Dimerization of endogenous IRF3 was examined by immunoblot analysis. Efficiency of TBK1-knockdown was determined by immunoblot analysis of S5 fractions (lower panel).

(D and E) Overexpression of RIG-I-N or MAVS directly activates IRF3. Reactions contained P5 of HEK293 cells transiently overexpressing Flag-RIG-I-N (D) or Flag-MAVS (E) without viral infection, and S5 of HEK293 cells without viral infection. Expression of Flag-tagged RIG-I-N or MAVS was determined by immunoblot analysis of cell homogenates (lower panel).

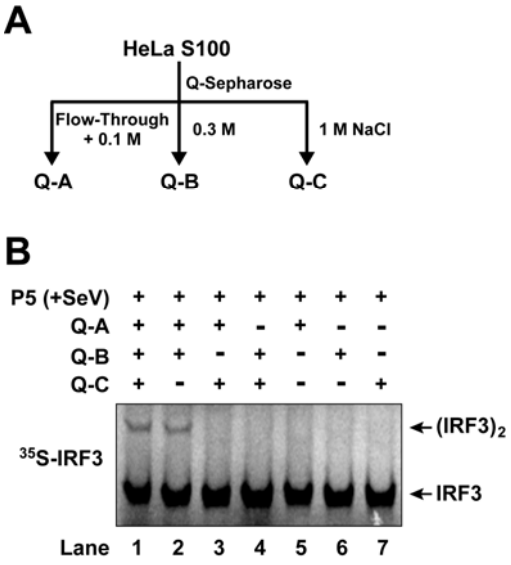

Figure 6. Separation of HeLa S100 into Two Active Fractions

(A) Fractionation of HeLa S100 on Q-Sepharose. Q-Sepharose column was sequentially eluted with a step-gradient of 0.1 M, 0.3 M and 1.0 M NaCl as described in **Experimental Procedures**. Q-A was a combination of flow-through and 0.1 M fraction, whereas 0.3 M and 1.0 M fractions gave rise to Q-B and Q-C, respectively.

(B) Reconstitution of IRF3 activation with Q-Sepharose fractions. *In vitro* assay for IRF3 activation was set up as in Fig. 4B with P5 of HEK293-MAVS cells with viral infection, and indicated combination of Q-A, Q-B and Q-C.

Ubc5 Is an Essential Component for Viral Activation of IRF3

Establishment of the robust assay makes it possible to identify new component(s) mediating viral activation of IRF3 through biochemical fractionation. In a pilot experiment, S100 prepared from HeLa cells was firstly applied to anion exchange column (Q-Sepharose), with three fractions recovered in a step-gradient of NaCl elution, namely Q-A, Q-B and Q-C (Fig. 6A). Q-A contained all the proteins unable to bind to the Q column at 0.1 M NaCl, whereas Q-B and Q-C contained proteins eluted from the column with 0.3 M and 1.0 M NaCl, respectively. In various combinations of the three fractions, IRF3 dimerization was shown to require both Q-A and Q-B, but not Q-C (Fig. 6B),

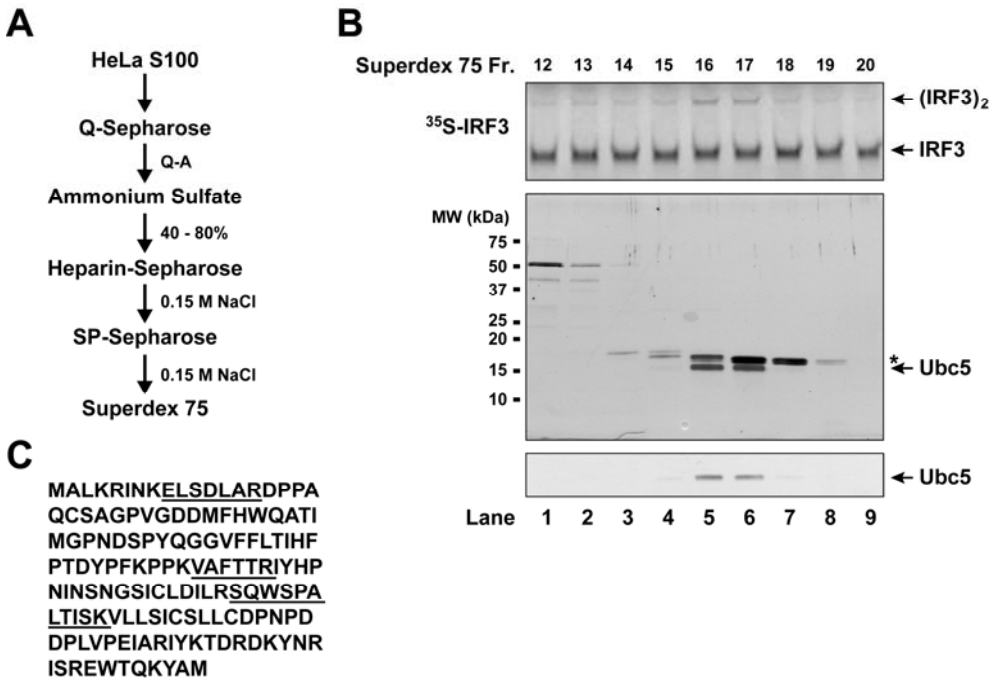

Figure 7. Identification of Ubc5 as Active Component in Q-A Fraction

(A) Scheme of biochemical fractionation of Q-A. Chromatography procedures were carried out as described in **Experimental Procedures**.

(B) Identification of Ubc5 as active component in Q-A. *In vitro* assay for IRF3 activation was set up as in Fig. 4B with P5 of HEK293-MAVS cells with viral infection, Q-B fraction as defined in Fig. 6A, and indicated gel-filtration fractions of Superdex-75 (upper panel). Aliquots of the same fractions were subjected to SDS-PAGE followed by silver staining (middle panel). Co-purification of Ubc5 with IRF3-activating activity was confirmed by immunoblot analysis (lower panel). The asterisk (*) in silver-stained gel denotes an irrelevant protein, cyclophilin A.

(C) Amino acid sequence of Ubc5c. Peptides recovered in mass spectrometry were underlined.

suggesting at least two distinct components involved in the reaction.

I focused on the activity in Q-A. This fraction was further subjected to five more steps of conventional chromatography as outlined in Fig. 7A. After each step of chromatography, IRF3-activating activity of each fraction was monitored

by *in vitro* assay supplemented with Q-B fraction, which presumably supplied several known component in this pathway including TBK1 and NEMO (data not shown). After the final fractionation by gel filtration, IRF3 dimerization activity showed a single peak at fractions 16 and 17 (Fig. 7B, upper panel), which on the silver-stained gel correlated with a protein band of an apparent molecular weight of 15 kDa (Fig. 7B, middle panel). Mass spectrometry analysis of the excised band identified three peptides corresponding to Ubc5b and/or Ubc5c (Fig. 7C), two of the three isoforms of Ubc5 in human genome. Co-purification of Ubc5 with IRF3-activating activity was further illustrated by immunoblot analysis with Ubc5 antibody (Fig. 7B, lower panel). Ubc5b and Ubc5c are the predominant isoforms of Ubc5 in most human cell lines (Jensen et al., 1995), and the antibody used for immunoblot could not distinguish these isoforms. However, it is conceivable that they could function redundantly in IRF3 activation, a notion supported by the finding that all three isoforms of Ubc5 activated IRF3 similarly *in vitro* (see below).

To confirm Ubc5 as the active component present in Q-A fraction, recombinant Ubc5 proteins were examined in a series of assays to substitute Q-A fraction. Recombinant Ubc5c efficiently supported the formation of IRF3 dimer,

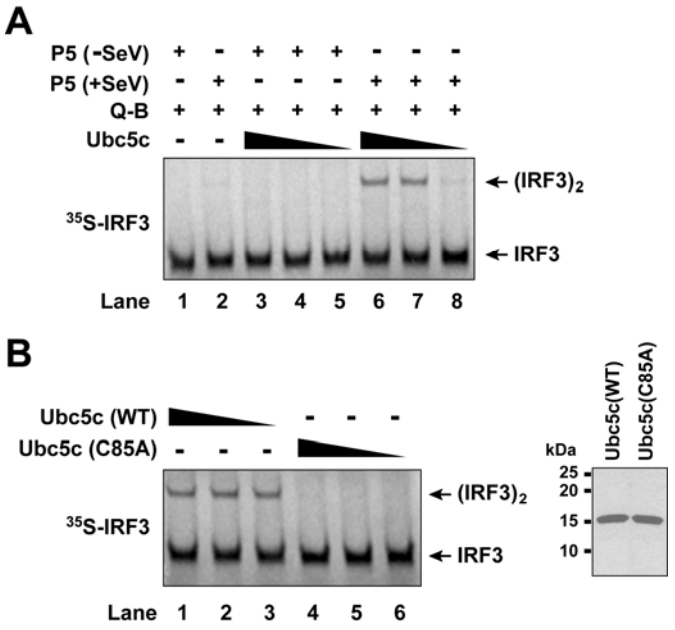

Figure 8. Ubc5 Is Sole Active Component in Q-A Fraction

In vitro assay for IRF3 activation was set up as in Fig. 4B.

(A) Substitution of Q-A fraction by recombinant Ubc5. Reactions contained indicated P5 of HEK293-MAVS cells without (-SeV) or with (+SeV) viral infection, Q-B as defined in Fig. 6A, and varying concentrations (0.1 -1 μM) of Ubc5c.

(B) Catalytic activity of Ubc5 is required for IRF3 activation. Reactions contained P5 of HEK293-MAVS cells with viral infection, Q-B as defined in Fig. 6A, and varying concentrations (0.1 - 1 μM) of recombinant Ubc5c WT, or catalytically inactive C84A-mutant. Protein quality of Ubc5c WT and C84A-mutant was examined by SDS-PAGE followed by Coomassie Blue staining (right panel).

which was dependent on viral-activated P5 in a same manner as Q-A fraction (Fig. 8A). Furthermore, the catalytic activity of Ubc5 was essential for its function, since a mutation of active-site cysteine of Ubc5c (C85A) completely abolished its ability to activate IRF3 (Fig. 8B).

To explore the specificity of Ubc5 in IRF3 activation, several widely-used members of E2 ubiquitin-conjugating enzyme family were tested, including E2-25K, Ubc3, Ubc5(a/b/c), Ubc7, and Ubc13/Uev1a. Surprisingly, only three isoforms of Ubc5 could substitute Q-A fraction to activate IRF3 (Fig. 9A),

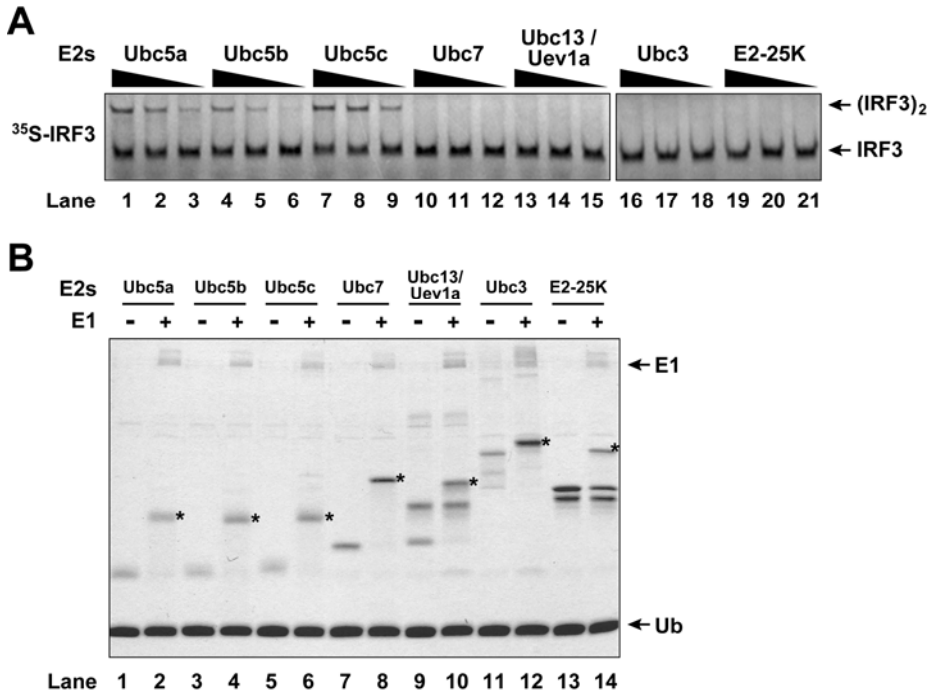

Figure 9. Ubc5 Functions a Specific E2 for IRF3 Activation

(A) Ubc5 as specific E2 for IRF3 activation. Reactions were set up as in Fig. 4B, containing P5 of HEK293-MAVS cells with viral infection, Q-B as defined in Fig. 6A, and varying concentrations (0.1 - 1 μM) of indicated E2s.

(B) Catalytic activity of E2s. Same set of E2s in (A) was analyzed for catalytic activity to form thioester with ubiquitin in the absence or presence of E1. Asterisks (*) denote the positions of individual E2-ubiquitin-thioester as visualized in Coomassie Blue stained gel.

indicating a specific role of Ubc5 in IRF3 activation. As a control for enzymatic activity, all the recombinant E2s were shown to form thioesters with ubiquitin in the presence of E1 and ATP (Fig. 9B).

Ubc5 Is Required for IRF3 Activation Upon Viral Infection

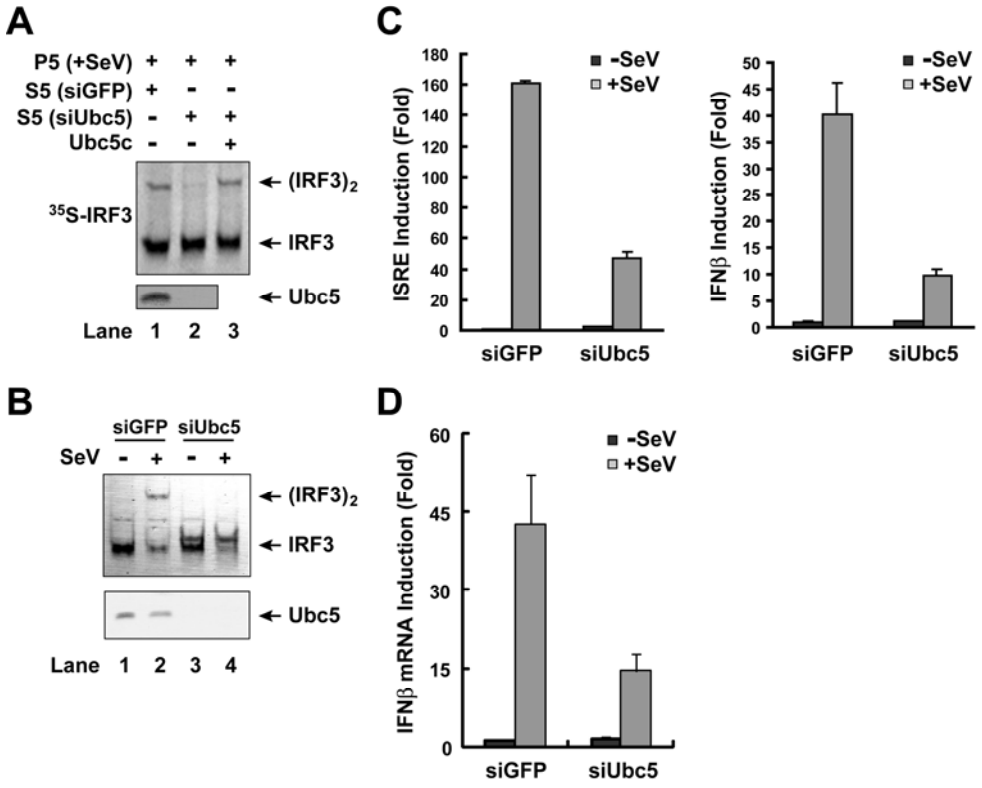

Figure 10. Ubc5 Is Required for IRF3 Activation

(A) Dependence of Ubc5 for IRF3 activation *in vitro*. Reactions were set up as in Fig. 4B, containing P5 of HEK293-MAVS cells with viral infection, and S5 of HEK293 cells transfected by siRNA against GFP or Ubc5. Efficiency of Ubc5-knockdown was determined by immunoblot analysis of S5 fractions (lower panel).

(B to D) Ubc5 is required for viral activation of IRF3 in cells. HEK293 cells were transfected with siRNA against GFP or Ubc5, together with luciferase reporters driven by ISRE- or IFNβ-promoter (C) as described in **Experimental Procedures**. Cells were treated without or with Sendai virus for 16 hours before dimerization of endogenous IRF3 (B), luciferase activity (C), or induction of IFNβ mRNA (D) was determined. Efficiency of Ubc5-knockdown was determined by immunoblot analysis of cell lysates (B, lower panel).

To determine whether Ubc5 is indeed an essential component to activate IRF3, Ubc5 was depleted and IRF3 activation was examined *in vitro* and also *in*

vivo in response to viral infection. Firstly, cytosolic extracts from HEK293T cells depleted of Ubc5 by RNAi failed to support IRF3 activation *in vitro* in the presence of mitochondria fraction from viral infected cells. And the deficiency was fully restored by adding back recombinant Ubc5c (Fig. 10A), indicating Ubc5 is required for IRF3 activation *in vitro*. Consistently, when endogenous Ubc5 in HEK293T cells was depleted by RNAi, it resulted in a) severely diminished induction of luciferase-reporter driven by interferon-stimulated response element (ISRE, an indicative of IRF3 activation), b) impaired induction of luciferase-reporter driven by IFNβ-promoter, and c) decreased IFNβ mRNA level, in response to viral infection (Fig. 10B and 10C). These data support the essential role of Ubc5 in viral-induced IRF3 activation.

To further confirm the requirement of Ubc5 for IRF3 activation by viral infection, and importantly, to determine if the catalytic activity of Ubc5 is necessary for IRF3 activation, a separate strategy was employed to deplete endogenous Ubc5 and simultaneously replace it with wildtype Ubc5c or the catalytic inactive form Ubc5c (C85A). Dr. Ming Xu constructed stable human osteosarcoma U2OS stable cell lines with tetracycline-inducible shRNA-knockdown of Ubc5b/c (Fig. 11A and B). In tetracycline-treated

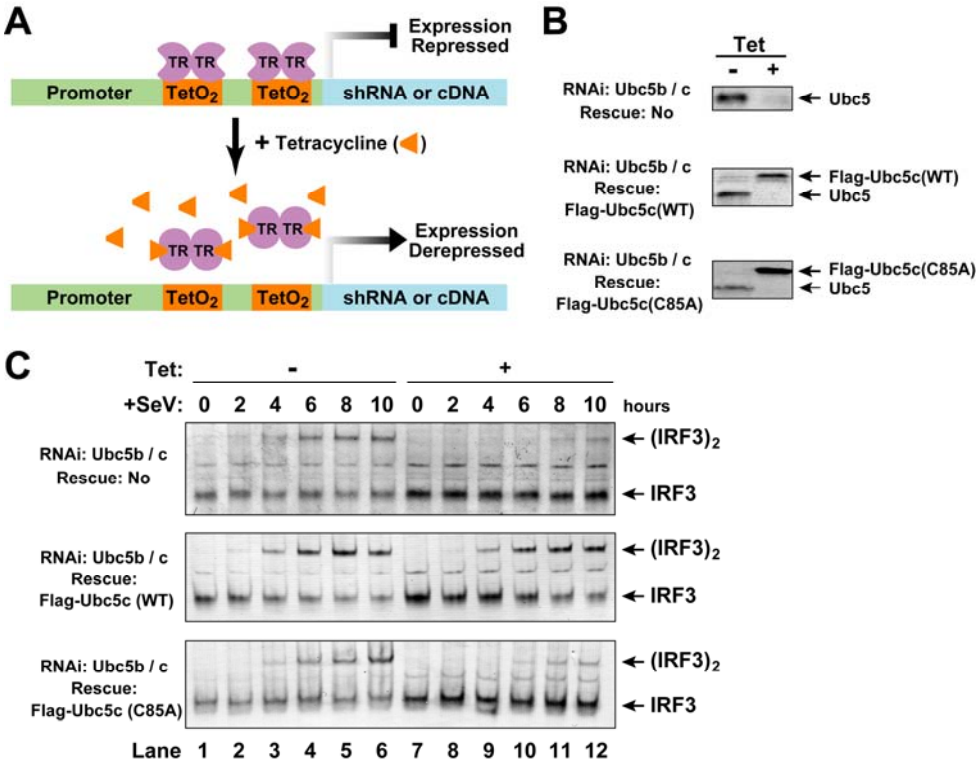

Figure 11. Catalytic Activity of Ubc5 Is Required for Viral Activation of IRF3

(A) Diagram of tetracycline-inducible shRNA-knockdown or rescue strategy. In the absence of tetracycline ligand, dimer of tetracycline-repressor (TR) bind to each of the two $TetO_2$ sites engineered in promoter region, repressing expression of downstream shRNA or cDNA. Upon addition of tetracycline, TR-dimer undergoes conformational change, and dissociates from $TetO_2$ sites, de-repressing expression of downstream shRNA or cDNA.

(B and C) Ubc5 is required for IRF3 activation upon viral infection. U2OS stable cell lines were cultured and treated with tetracycline (Tet) as described in **Experimental Procedures**. Indicated U2OS-Ubc5b/c cells without rescue, or rescued by siRNA-resistant Flag-Ubc5c(WT) or Flag-Ubc5c(C85A) were infected by SeV for 0 to 10 hours. Dimerization of endogenous IRF3 was examined by immunoblot analysis (C). Efficiency of tetracycline treatment on depletion of endogenous Ubc5 and expression of exogenous siRNA-resistant Flag-Ubc5c proteins was determined by immunoblot analysis of cell lysates (B).

Ubc5b/c-knockdown cells, endogenous Ubc5 was dramatically reduced,

viral-stimulated IRF3 dimerization was significantly delayed compared to mock treated cells (Fig. 11C). Consistent with impaired activation of IRF3, IFNβ production in Ubc5b/c-knockdown cells was also blocked (Fig. 12A). The final appearance of IRF3 dimer at late time points (8 to 10 hours) and a small amount of IFNβ production in Ubc5b/c-knockdown cells could be explained by residual amount of Ubc5 protein remaining in the cells (Fig. 11B). To exclude the off-target effect of shRNA, the defective response to viral infection in Ubc5b/c-knockdown cells could be efficiently rescued by tetracycline-inducible expression of siRNA-resistant Flag-Ubc5c(WT), but not a comparable level of catalytic inactive Flag-Ubc5c(C85A) (Fig. 11C and Fig. 12A). The rescue experiments re-affirmed the finding that catalytically active Ubc5 was required by viral activation of IRF3. Moreover, knockdown of Ubc5b/c efficiently blocked IRF3 activation induced by exogenous overexpression of MAVS (Fig. 12B), supporting the function of Ubc5 downstream of MAVS. Taken together, I provided several lines of evidence that Ubc5 is a key component downstream of MAVS in viral activation of IRF3.

Involvement of Lys63-Linked Polyubiquitination in IRF3 Activation

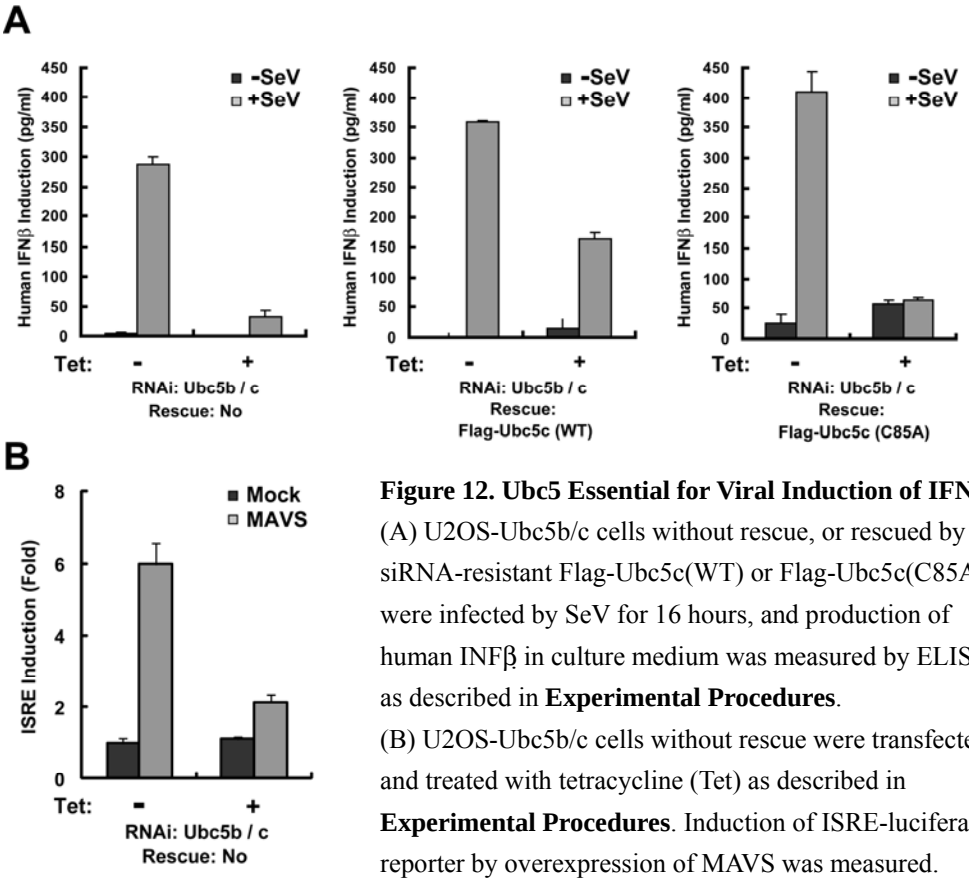

Figure 12. Ubc5 Essential for Viral Induction of IFNβ
(A) U2OS-Ubc5b/c cells without rescue, or rescued by siRNA-resistant Flag-Ubc5c(WT) or Flag-Ubc5c(C85A) were infected by SeV for 16 hours, and production of human INFβ in culture medium was measured by ELISA as described in **Experimental Procedures**.
(B) U2OS-Ubc5b/c cells without rescue were transfected, and treated with tetracycline (Tet) as described in **Experimental Procedures**. Induction of ISRE-luciferase reporter by overexpression of MAVS was measured.

The requirement for catalytic activity of Ubc5 in viral activation of IRF3 immediately implied a role of polyubiquitination in the process. Two major forms of ubiquitin-chain linkage (K48- and K63-linked) have been extensively studied, K48-linked polyubiquitination is widely involved in proteasome-mediated protein degradation, and K63-linked polyubiquitination is indicated in signal transduction through a non-proteolytic mechanism. It was important to determine the specific linkage involved in IRF3 activation to understand the potential mechanism. The

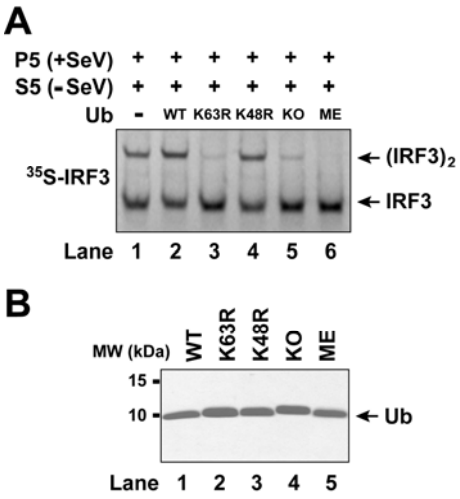

Figure 13. K63-Linked Ubiquitination Is Involved in IRF3 Activation *In Vitro*
(A and B) K63-linked ubiquitination in IRF3 activation. *In vitro* assay for IRF3 activation was set up as in Fig. 4B, containing P5 of HEK293 cells with viral infection, S5 of HEK293 cells without viral infection, and indicated versions of recombinant ubiquitin proteins (A). Protein quality of ubiquitin proteins used in (A) was examined by SDS-PAGE followed by Coomassie Blue staining (B).

biochemical assay for IRF3 dimerization was partly based on crude fractions (i.e., P5 and Q-B), it remained difficult to directly examine the nature of ubiquitin-chain formed *in vitro*. Therefore, in an alternative way, I sought to observe the dominant-negative effect of recombinant ubiquitin mutant proteins purified from *E. coli* (Fig. 13B). When recombinant ubiquitin wild-type or K48R-mutant was added in the assays, formation of IRF3 dimer was not affected. However, IRF3 dimerization was strongly inhibited by the addition of K63R, No-Lys (KO) or Methylated (ME) ubiquitin (Fig. 13A), indicating that K63- but not K48-linked polyubiquitination was involved in IRF3 activation.

Previous studies have documented the critical roles of K63-linked polyubiquitination in signaling transduction (Chen and Sun, 2009), e.g., IκB

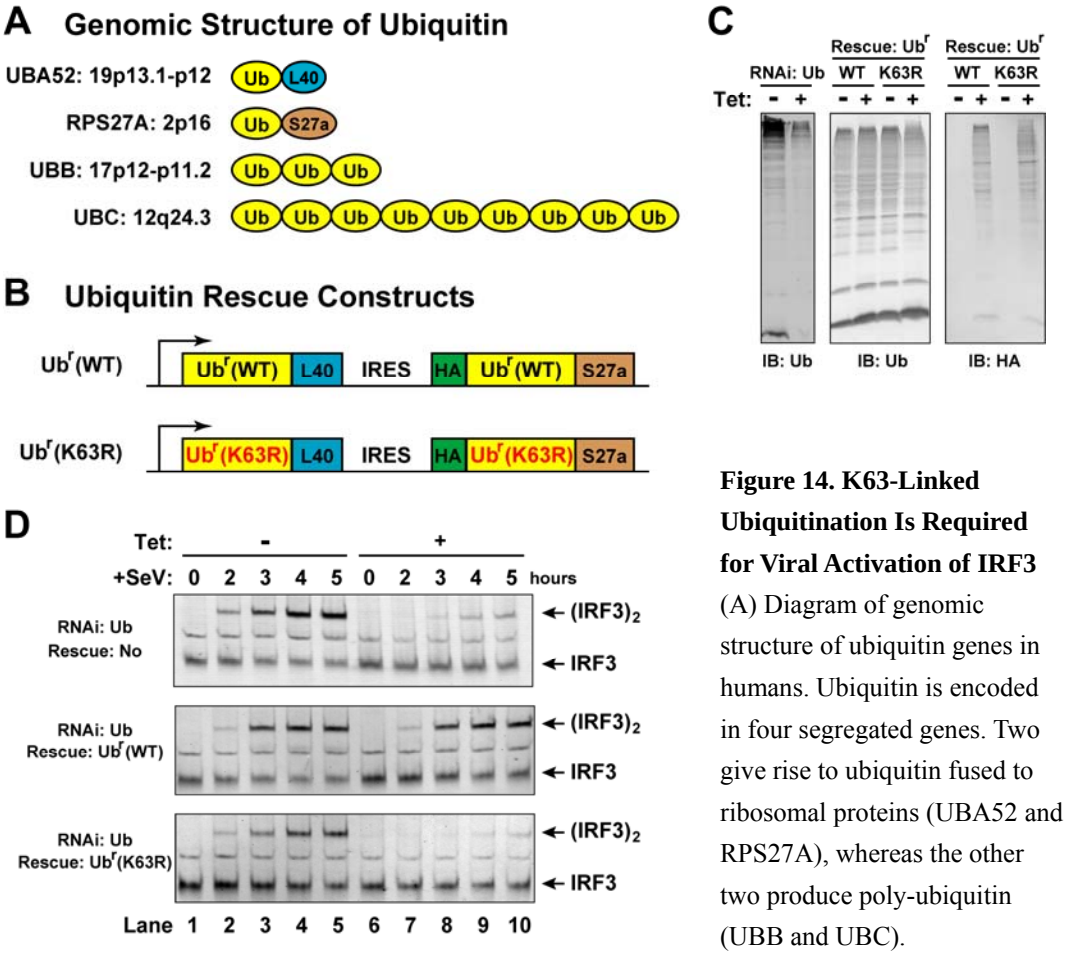

Figure 14. K63-Linked Ubiquitination Is Required for Viral Activation of IRF3

(A) Diagram of genomic structure of ubiquitin genes in humans. Ubiquitin is encoded in four segregated genes. Two give rise to ubiquitin fused to ribosomal proteins (UBA52 and RPS27A), whereas the other two produce poly-ubiquitin (UBB and UBC).

(B) Strategy to generate siRNA-resistant ubiquitin (Ub^r) for rescue constructs.

(C and D) K63-linked polyubiquitination is essential for IRF3 activation upon viral infection. Indicated U2OS-Ub stable cells without rescue, or rescued by Ub^r(WT) or Ub^r(K63R) were infected by SeV for 0 to 5 hours, and dimerization of endogenous IRF3 was examined by immunoblot analysis (D). Efficiency of tetracycline treatment on depletion of endogenous Ub and expression of exogenous Ub^r proteins, with and without HA-tag, was confirmed by immunoblot analysis of cell lysates (C).

kinase activation. However, direct evidences for the specific linkage requirement *in vivo* were incomplete, largely due to the complexity of ubiquitin genes structure.

There are four known genes encoding ubiquitin precursors in human genomes (Fig. 14A), two of which are translated into linear poly-ubiquitin (UBB and UBC), and the other two produce ubiquitin fused to ribosomal subunits (UBA52 and RPS27A). Dr. Ming Xu employed the same strategy to Ubc5 inducible knockdown and constructed U2OS stable cells lines with tetracycline-inducible shRNA against ubiquitin, which could deplete endogenous ubiquitin to more than 80% (Fig. 14C). Furthermore, Dr. Ming Xu constructed rescue cell lines expressing both UBA52 and RPS27A encoding RNAi-resistant form of ubiquitin (Ub^r) wild type or K63R-mutant (Fig. 14B), and replenished the expression level of ubiquitin similar to that of untreated cells (Fig. 14C).

I took advantage of the ubiquitin-knockdown U2OS cells to explore the role of K63-linked polyubiquitination in viral activation of IRF3 *in vivo*. In tetracycline-inducible ubiquitin-knockdown cells, viral-induced dimerization of IRF3 was abolished compared to mock treatment. And the defect could be fully restored by exogenous expression of Ub^r wild-type (Fig. 14D), in support of the notion that ubiquitination was involved in IRF3 activation. Strikingly, replacement of endogenous ubiquitin with a comparable level of Ub^r K63R-mutant failed to rescue the IRF3 defect (Fig. 14D), emphasizing the finding

that K63-linked polyubiquitination was essential in viral activation of IRF3.

Ubiquitin-Binding Activity of NEMO Is Required for IRF3 Activation

K63-linked ubiquitin-chain has been documented to function as a scaffold for signaling components in IκB kinase activation (Adhikari et al., 2007). And it was tempting to hypothesize that a similar function of K63-polyubiquitination could underlie the mechanism for IRF3 activation. Interestingly, NEMO, a ubiquitin binding protein, was recently described as an essential component for MAVS-mediated IRF3 activation in viral-infected cells (Zhao et al., 2007). And it appeared as a promising candidate for further characterization.

Several domain structures have been characterized for NEMO (Fig. 15A). IKK-binding domain (KBD) contributes to the formation of NEMO/IKKα/IKKβ complex, and C-terminal region containing leucine-zipper motif (LZ) functions as ubiquitin-binding domain (Ea et al., 2006; Wu et al., 2006). Recently, zinc-finger domain (ZF) at the distal C-terminus has also been shown to exert ubiquitin-chain binding ability (Cordier et al., 2009). Virtually, GST-fused zinc-finger domain alone was sufficient for K63-linked ubiquitin-chain interaction (Fig. 15D).

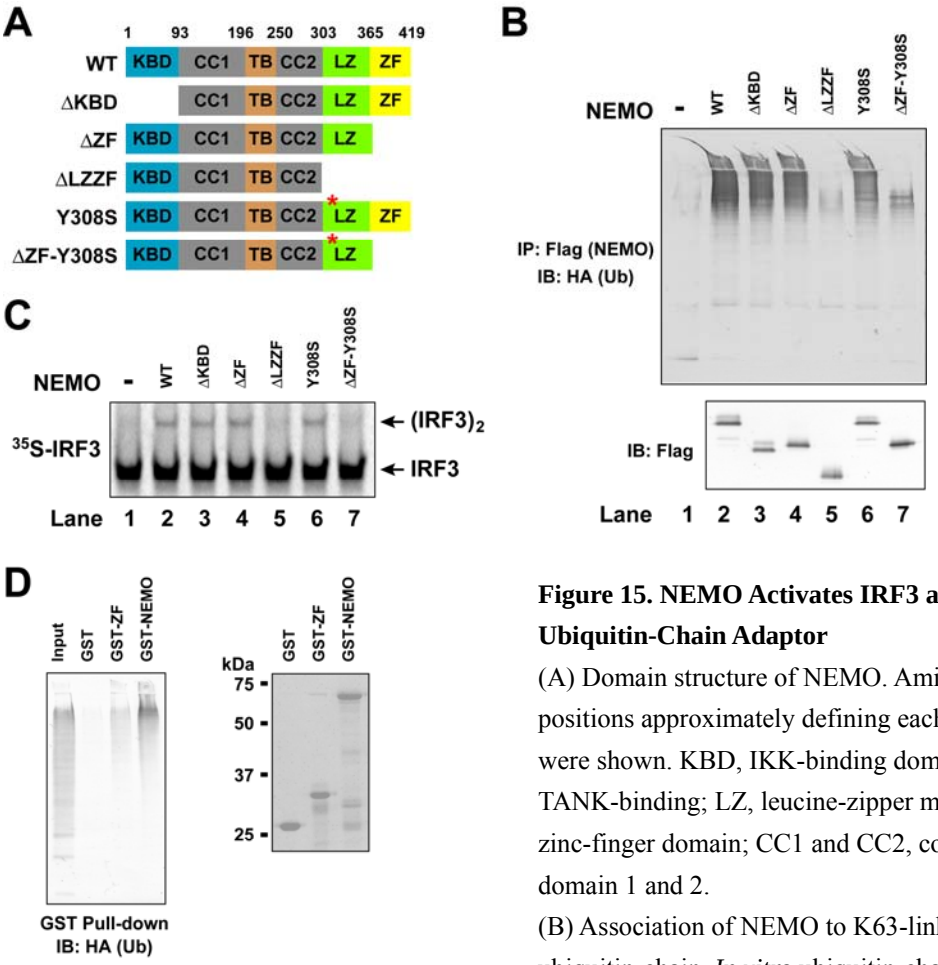

Figure 15. NEMO Activates IRF3 as Ubiquitin-Chain Adaptor

(A) Domain structure of NEMO. Amino-acid positions approximately defining each domain were shown. KBD, IKK-binding domain; TB, TANK-binding; LZ, leucine-zipper motif; ZF, zinc-finger domain; CC1 and CC2, coiled-coil domain 1 and 2.

(B) Association of NEMO to K63-linked ubiquitin-chain. *In vitro* ubiquitin-chain binding assay was carried out as described in **Experimental Procedures**.

(C) Ubiquitin-chain binding of NEMO is required for IRF3 activation *in vitro*. *In vitro* assay for IRF3 activation was set up as in Fig. 4B, containing P5 of HEK293 cells with viral infection, S5 of NEMO$^{-/-}$ MEF cells, and indicated versions of NEMO proteins purified as in (B).

(D) Ubiquitin-chain binding of zinc-finger domain of NEMO. GST-tagged NEMO and its zinc-finger domain were subjected to *in vitro* ubiquitin-chain binding assay. After glutathione-agarose pull-down, ubiquitin-chain was detected by immunoblot analysis (left panel). Quality of GST-tagged proteins was examined by SDS-PAGE followed by Coomassie Blue staining (right panel).

A series of mutant versions of Flag-tagged NEMO were purified from

transiently transfected HEK293T cells, including mutant forms with disrupted ubiquitin-binding ability. Consistent with previous reports, Flag-NEMO(WT) bound to K63-linked ubiquitin-chain strongly, and truncation of IKK-binding domain (ΔKBD) did not affect ubiquitin-binding (Fig. 15B, Lane 1 to 3). Either deletion of zinc-finger domain (ΔZF), or substitution of tyrosine-308 with serine residue (Y308S), which abolishes ubiquitin-binding of leucine-zipper motif, had mild effect on ubiquitin-chain association of the proteins (Fig. 15B, Lane 4 and 6). In contrast, destruction of both leucine-zipper motif and zinc-finger domain, i.e., NEMO(ΔLZZF) and NEMO(ΔZF-Y308S), dramatically decreased the interaction with K63-linked ubiquitin-chain (Fig. 15B, Lane 5 and 7). Thus, the evidences supported that leucine-zipper motif and zinc-finger domain of NEMO independently contributed to binding of K63-linked ubiquitin-chain.

Next, the requirement of ubiquitin-chain binding of NEMO in IRF3 activation was examined. The same set of mutant versions of NEMO was firstly tested in the biochemical assay with cytosol prepared from NEMO-deficient MEF cells, which was largely defective in IRF3 activation. IRF3 dimerization could be efficiently rescued by the addition of NEMO(WT), and also NEMO(ΔKBD), NEMO(ΔZF) and NEMO(Y308S) (Fig. 15C). However, correlating with their

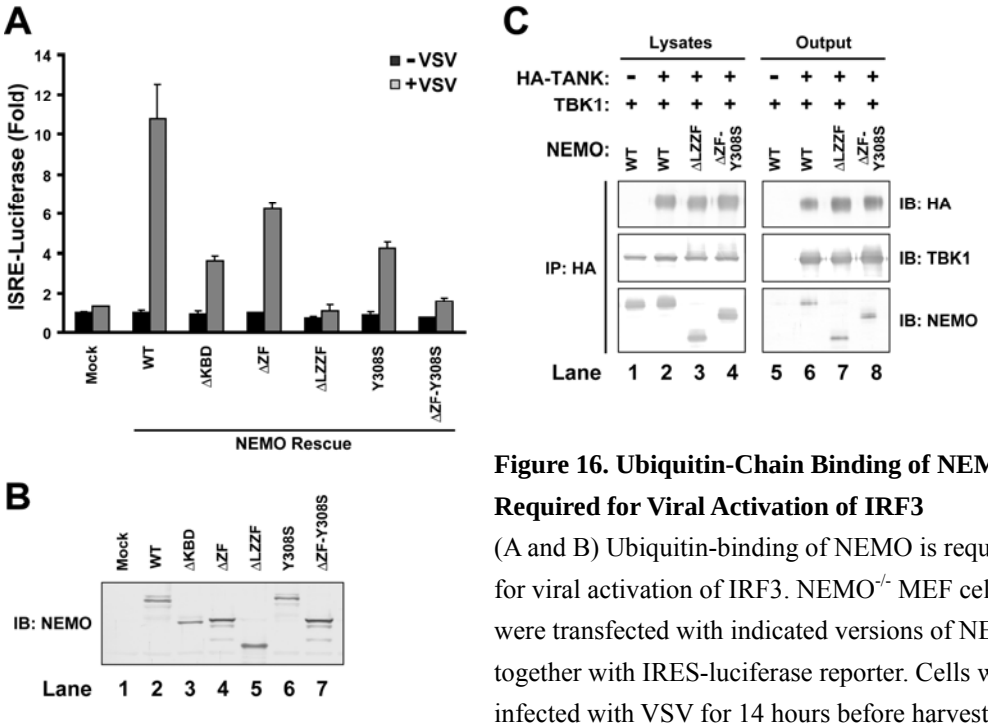

Figure 16. Ubiquitin-Chain Binding of NEMO Is Required for Viral Activation of IRF3

(A and B) Ubiquitin-binding of NEMO is required for viral activation of IRF3. NEMO$^{-/-}$ MEF cells were transfected with indicated versions of NEMO together with IRES-luciferase reporter. Cells were infected with VSV for 14 hours before harvested for measurement of luciferase activity (A). Expression of NEMO and its mutants was determined by immunoblot analysis of cell lysates (B).

(C) Normal interaction of TBK1/TANK with NEMO mutants. HEK293 cells were transfected with TBK1, TANK, and indicated versions of NEMO. Formation of TBK1/TANK/NEMO complex was determined by immune-precipitation followed by immunoblot analysis.

defects in ubiquitin-chain binding, NEMO(ΔLZZF) and NEMO(ΔZF-Y308S) failed to restore the activation of IRF3 (Fig. 15C). The same requirement for ubiquitin-chain binding of NEMO was also observed in NEMO-deficient MEF cells transfected with individual version of NEMO mutants. In ISRE-reporter assay, cells transfected with NEMO(ΔLZZF) or NEMO(ΔZF-Y308S) failed to respond to Vesicular Stomatitis Virus (VSV) infection, whereas similar expression

level of NEMO(WT) or other indicated mutants rescued the original defect to certain levels (Fig. 16A and B). To rule out the possibility that defects of NEMO(ΔLZZF) and NEMO(ΔZF-Y308S) were due to incapability to form NEMO/TANK/TBK1 complex, the two mutants were shown to be co-immunoprecipitated with TANK similar to NEMO(WT) (Fig. 16C). Taken together, these results suggesting that NEMO was involved in IRF3 activation possibly as a K63-linked ubiquitin-chain adaptor.

Towards Identification of E3(s) Involved in MAVS-Mediated IRF3 Activation

Since K63-linked polyubiquitination is essential for viral activation of IRF3, an obvious question was related to the identity of the specific ubiquitin-ligase E3(s) in the reaction. While we were still vigorously pursuing the fractionation of Q-B fraction in hope of uncovering the specific E3(s), I decided to take a candidate approach, alternatively.

Previous studies have implied the role of several E3 members belonging to TRIM and TRAF families in the pathway, e.g., TRIM25, TRAF3, and TRAF6 (Gack et al., 2007; Hacker et al., 2006; Oganesyan et al., 2006; Xu et al., 2005). In TRIM25-deficient MEF cells, a delayed IFNβ production to viral infection was

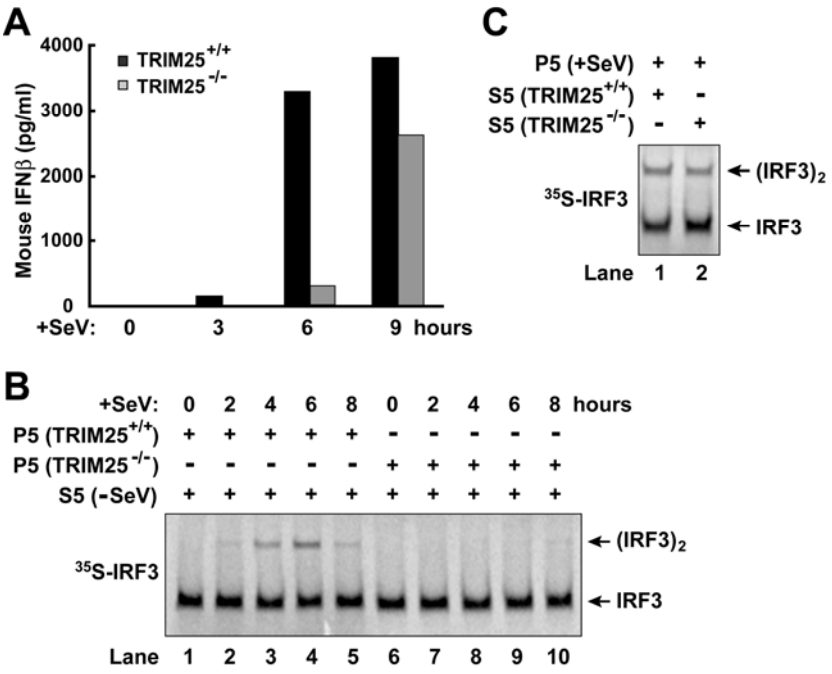

Figure 17. **TRIM25 Functions Upstream of MAVS in IRF3 Activation**
(A) Impaired IFNβ production in TRIM25$^{-/-}$ MEF cells. TRIM25$^{+/+}$ and TRIM25$^{-/-}$ MEF were infected with SeV for indicated times before mouse IFNβ produced in culture medium was measured by ELISA as described in **Experimental Procedures**.
(B and C) TRIM25 functions through MAVS in IRF3 activation. *In vitro* assay for IRF3 activation was set up as in Fig. 4B, containing indicated P5 of TRIM25$^{+/+}$ or TRIM25$^{-/-}$ MEF cells infected with SeV for 0 to 8 hours, and S5 of HEK293 cells without viral infection (B), or P5 of HEK293 cells with viral infection, and S5 of TRIM25$^{+/+}$ or TRIM25$^{-/-}$ MEF cells (C).

observed compared to TRIM25$^{+/+}$ cells (Fig. 17A). In accordance with its role as E3 for ubiquitination and activation of RIG-I, mitochondria (P5) isolated from viral-infected TRIM25$^{-/-}$ cells failed to support IRF3 dimerization in the *in vitro* assay (Fig. 17B). In contrast, in the presence of viral-activated P5, cytosol (S5) fractions from TRIM25$^{-/-}$ and TRIM25$^{+/+}$ cells were indistinguishable in the ability

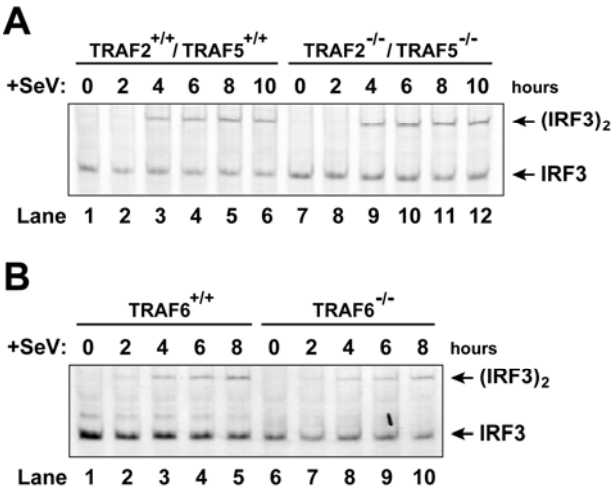

Figure 18. Viral Activation of IRF3 in TRAF2$^{-/-}$/TRAF5$^{-/-}$ and TRAF6$^{-/-}$ MEF cells

(A and B) Indicated MEF cells were infected by SeV for 0 to 10 hours (A), or 0 to 8 hours (B). Dimerization of endogenous IRF3 was examined by immunoblot analysis.

for IRF3 activation (Fig. 17C). Therefore, it was very likely that TRIM25 functions on RIG-I, but not downstream of MAVS in signaling pathway.

TRAF2 and TRAF5, two other TRAF family members previously indicated in K63-linked polyubiquitination synthesis and IKK activation (Bradley and Pober, 2001) were also explored to determine their involvement in this pathway. In TRAF2$^{-/-}$/TRAF5$^{-/-}$ double-deficient MEF cells, viral infection resulted in a rapid appearance of endogenous IRF3 dimer, same as that in TRAF2$^{+/+}$/TRAF5$^{+/+}$ cells (Fig. 18A). Similarly, no defect of IRF3 dimerization was observed in TRAF6-deficient cells upon viral infection (Fig. 18B). Although the evidences failed to support any direct role of TRAF2, TRAF5 or TRAF6 in viral activation of IRF3, a possibility of functional redundancy among those E3s could not

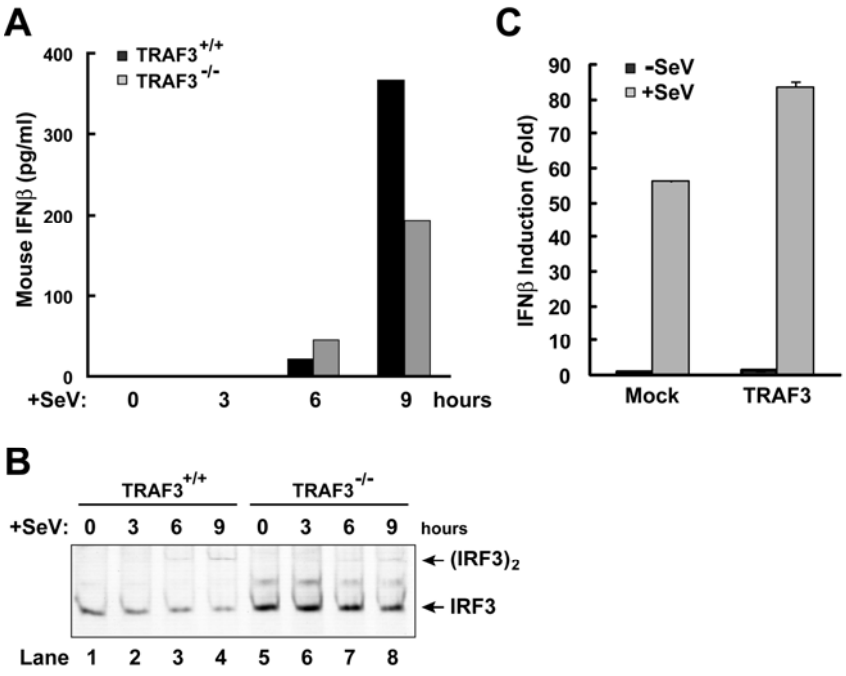

Figure 19. TRAF3 Is Involved in IRF3 Activation

(A) Mild decrease of IFNβ production in TRAF3$^{-/-}$ MEF cells. Cells were infected with SeV for indicated times before mouse IFNβ produced in culture medium was measured by ELISA.

(B) IRF3 activation in TRAF3$^{+/+}$ and TRAF3$^{-/-}$ MEF. Cells were infected by SeV for 0 to 9 hours, and dimerization of endogenous IRF3 was examined by immunoblot analysis.

(C) Overexpression of TRAF3 enhances IFNβ induction upon viral infection. HEK293 cells were transfected with mock vector or TRAF3, and infected by SeV for 16 hours before induction of IFNβ mRNA was determined.

currently be ruled out.

Upon viral infection in TRAF3-deficient MEF cells, a modest reduction of IFNβ production was detected (Fig. 19A), together with a mild decrease of IRF3 dimerization (Fig. 19B). Moreover, transient overexpression of TRAF3 in HEK293T cells sensitized the viral response, shown as a 50% increase in

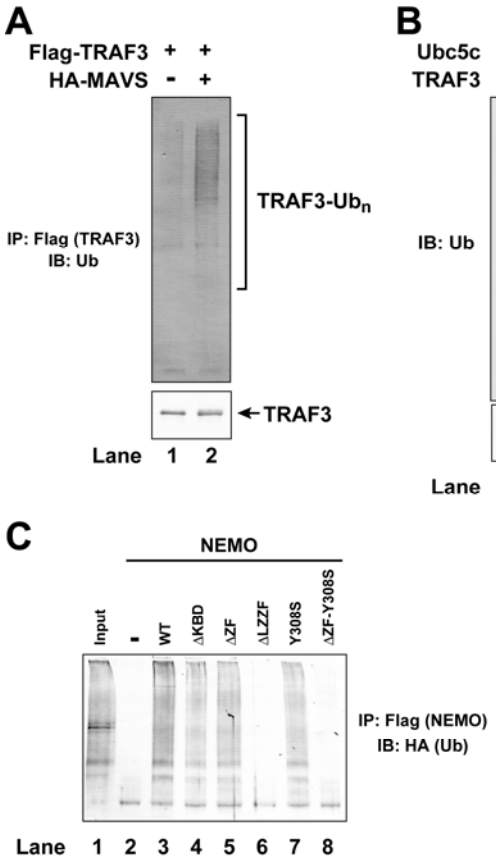

Figure 20. Possible Role of TRAF3 in Viral Activation of IRF3

(A) MAVS-mediated ubiquitination of TRAF3. HEK293 cells were transfected with Flag-TRAF3 without or with MAVS. Following immune-affinity purification of TRAF3, ubiquitination of the protein was examined by immunoblot analysis.

(B) Ubc5 supports ubiquitin-chain synthesis catalyzed by TRAF3. *In vitro* ubiquitination reaction was carried out as described in **Experimental Procedures**.

(C) Binding of NEMO to ubiquitin-chain synthesized by TRAF3. *In vitro* ubiquitin-chain binding assay was carried out as in Fig. 15B, with ubiquitin-chain synthesized by Ubc5 and TRAF3.

IFNβ induction by reporter assay (Fig. 19C). Thus, it appeared that TRAF3 might function as one component in IRF3-activating pathway. TRAF3 has been the most extensively studied candidate in the pathway, and previous studies have suggested the role of TRAF3 in interferon induction upon viral infection (Hacker et al., 2006; Oganesyan et al., 2006; Saha et al., 2006). Here, several lines of evidences further support a role of TRAF3 in IRF3 activation. Firstly, endogenous TRAF3 showed

MAVS-dependent auto-ubiquitination (Fig. 20A). Secondly, TRAF3 could form ubiquitin-chain efficiently with Ubc5 (Fig. 20B). Finally, NEMO potently associate with ubiquitin-chain synthesized by Ubc5 and TRAF3, and the interaction depended on the two ubiquitin-binding domains of NEMO (Fig. 20C). However, as pointed out above, it remained an open question whether TRAF3 functions redundantly with other E3(s) in the pathway, which could explain the only modest defect in TRAF3$^{-/-}$ cells.

As another approach to search for potential E3(s) involved in the ubiquitination process, RNA interference (RNAi) screening was initially performed. QIAGEN siRNA library against about 600 E3s in human genomes was used to knock down individual E3 followed by viral infection and IFNβ induction measurement using IFNβ-luciferase reporter assay (Fig. 21). Positive hits were selected according to the criterion that knockdown of these genes decreased IFNβ induction to more than 50%. The candidates from the primary screening were further applied to second round of screening to narrow down the list functioning downstream of RIG-I and upstream of TBK1. Briefly, RIG-I-N and TBK1 were overexpressed in HEK293T cells following siRNA knockdown of these individual E3 separately. Positive hits were selected based on the criterion

	1	2	3	4	5	6	7	8	9	10
A	CBLB	TRIM68	MGRN1	PSMA5	RBBP6	HSF4	MAR4	RAPSN	MAR2	UBR1
B	CISH	TRIM62	TRIM34	RNF121	FBXL2	KCNC4	TRIM11	HERC3	MDM2	KCNG1
C	KCNA4	HECTD3	WSB2	KCTD16	FBXL3	PSMA3	TRIM63	HUWE1	PSMA6	VHL
D	TRAF5	UBE3B	TRIM7	ZBTB46	STMN3	HERC2	BTBD6	RBCK1	PSMD7	TRIM10
E	TRIM25	TRIM64	RNF183	KCTD6	BTBD7	PARC	ZBTB9	ZBTB43	ARIH2	CGRRF1
F	TRAF4	PSMA1	BMI1	KLHL17	NEURL2	FBXO28	ZBTB12	MKRN2	UBOX5	ZBTB20
G	PPIL2	PSMA4	KCNA6	PML	SH3RF2	RNF17	RNF182	FBXL5	KCTD9	LRRC29
H	RNF12	RING1	PSMA2	PSMB4	LOC388419	KLHL8	KLHL30	RNF141	BIRC7	LNX2

Figure 21. Summary of siRNA Screening of Human E3 Library
HEK293T cells stably expressing IFNβ-luciferase and pCMV-(Renilla luciferase) reporters were transfected with set of siRNAs against individual E3 as described in **Experimental Procedures**. Induction of IFNβ-luciferase reporter was measured 16 hours post viral infection, and siRNA-knockdown of listed genes inhibited IFNβ-reporter by more than 50%. siRNA-knockdown of color-shaded genes suppressed IFNβ-reporter induced by overexpression of RIG-I-N by more than 50%, but did not block that induced by overexpression of TBK1.

that knockdown of these genes blocked IFNβ induction by overexpressed RIG-I-N but not by TBK1. By testing a dozen of most promising hits, no candidate was shown to work specifically in the pathway (data not shown).

Viral-Induced Ubiquitination of MAVS

Besides E3 (s), the target(s) for direct ubiquitin-chain linkage was also unknown. Since TRAF3 showed signal-dependent polyubiquitination (Fig. 20A),

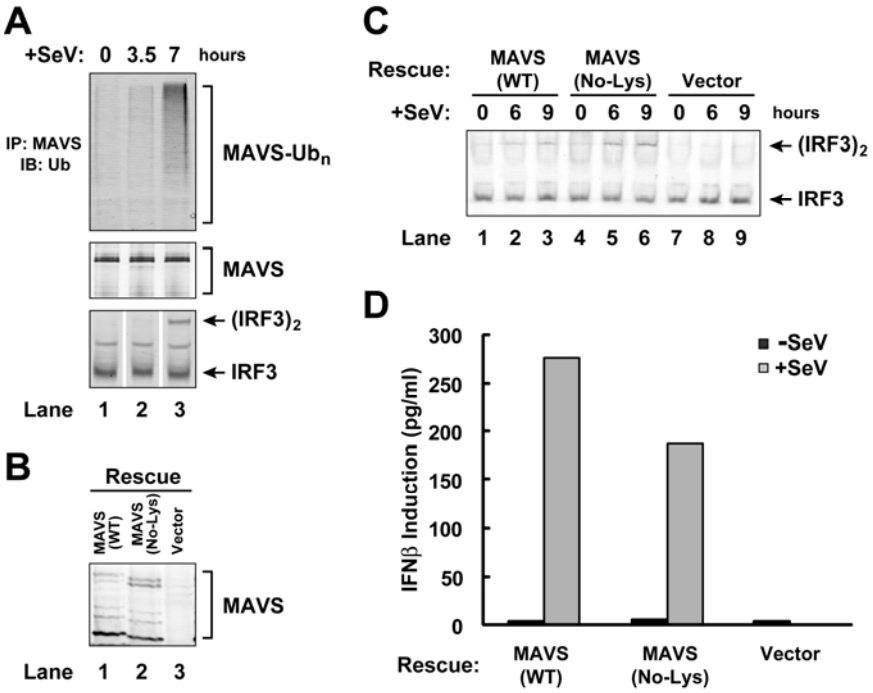

Figure 22. Ubiquitination of MAVS in Response to Viral Infection

(A) Ubiquitination of MAVS correlates with IRF3 activation. HEK293 cells were infected by SeV for 0 to 7 hours, and dimerization of endogenous IRF3 was examined by immunoblot analysis (lower panel). Ubiquitination of endogenous MAVS was determined following immune-precipitation (Upper panel).

(B to D) Ubiquitination of MAVS is not essential for viral activation of IRF3. MAVS$^{-/-}$ MEF cells without rescue, or rescued by MAVS(WT) or MAVS(No-Lys) were infected by SeV for 0 to 9 hours, and dimerization of endogenous IRF3 was examined by immunoblot analysis (C). In parallel, production of mouse IFNβ in indicated MEF cells was measured by ELISA (D). Exogenous expression of MAVS proteins in MEF cells was determined by immunoblot analysis of cell lysates (B).

it remained to be explored whether TRAF3 itself could serve as ubiquitination target in the process.

Another possible target was MAVS, robust polyubiquitination of which was

observed upon viral infection (Fig. 22A, upper panel). Also, the ubiquitination process of MAVS correlated with the appearance of IRF3 dimer (Fig. 22A, lower panel). Moreover, mass spectrum analysis of immuno-precipitated MAVS from viral infected cells unambiguously determined that the protein was targeted by K63-linked polyubiquitination (data not known). To examine whether ubiquitination of MAVS could possibly function in activation of IRF3, a mutant version of MAVS in which all 15 Lys residues were substituted by Arg was introduced back to MAVS-deficient MEF cells. Compared with the cells rescued by MAVS(WT), a comparable expression level of MAVS(No-Lys) also restored the defect of IRF3 activation upon viral infection (Fig. 22B and C). Consistently, expression of MAVS(No-Lys) resulted in a robust induction of IFNβ (Fig. 22D). Taken together, it is unlikely that ubiquitination of MAVS is directly involved in viral activation of IRF3.

Model for MAVS-Mediated IRF3 Activation

Based on current evidence, a working model is proposed for MAVS-mediated IRF3 activation (Fig. 23). Briefly, viral activation of MAVS promotes the protein oligomerization, which might function to recruit a

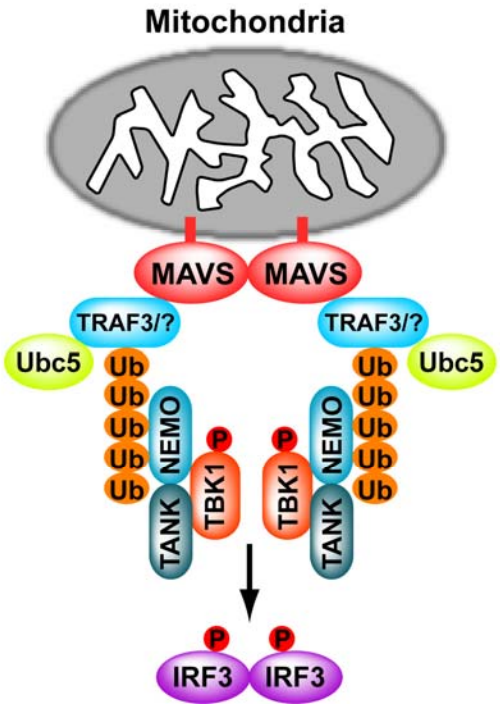

Figure 23. Model for MAVS-Mediated IRF3 Activation through K63-Linked Polyubiquitination

Viral infection leads to oligomerization of MAVS on mitochondrial. Viral-activated MAVS then recruits TRAF3 and possibly other ubiquitin ligase(s), which function together with Ubc5 to catalyze K63-linked polyubiquitination on TRAF3 or other target protein(s). Ubiquitin-chains help to recruit NEMO, which in turn interacts with TANK and TBK1. Upon trans-activation through phosphorylation, TBK1 finally phosphorylates its substrate IRF3.

ubiquitin-ligase E3 (e.g., TRAF3). Together with Ubc5 as specific ubiquitin-conjugating E2, K63-polyubiquitin chains are synthesized and directly conjugated to a substrate, one possibility of which is the E3 itself. Through ubiquitin-binding domains of NEMO, association of TBK1/TANK/NEMO complex with K63-linked ubiquitin-chains then probably results in trans-activation of TBK1, which finally phosphorylates IRF3.

Conclusion of Research Project

In summary, my current study has unveiled a novel mechanism of MAVS-mediated IRF3 activation through K63-polyubiquitination, which will facilitate further investigation into the regulatory activation of IRF3 and other IRFs in innate immunity.

CHAPTER III: DISCUSSION

In current study, a cell-free system was employed to explore the mechanism by which MAVS transduces signal upon viral infection to activate IRF3. I provided evidences that such a biochemical assay *in vitro* recapitulated the phosphorylation and dimerization of IRF3, and faithfully reflected epistatic interactions of the known components in the signaling cascade. With this robust assay, I successfully carried out conventional fractionation procedures, and identified Ubc5 as a specific ubiquitin-conjugating enzyme required for IRF3 activation. Furthermore, combining RNAi-knockdown strategy in culture cells, an essential role of K63-linked polyubiquitination in viral activation of IRF3 was demonstrated. Finally, evidence was presented to show that NEMO might function as a K63-linked ubiquitin-chain adaptor required for transducing signals to TBK1 to phosphorylate IRF3. .

K63-Linked Polyubiquitination in Signaling

Besides numerous studies of K48-linked polyubiquitination in regulating destruction of key cell components in various signaling pathways, the last decade

has seen a surge in functional demonstrations of polyubiquitination in proteasome-independent events, particularly the involvement of K63-linked conjugation in signaling cascades (Chen and Sun, 2009). It has been generally believed that structural difference between K48- and K63-linked polyubiquitination is the main explanation to their distinct roles in cell signaling. Crystallographic data have revealed that these two forms of ubiquitin-chain expose different surface residues of ubiquitin monomer, and also have difference in overall topology (Tenno et al., 2004; Varadan et al., 2004), which could result in specific recognition by downstream adaptors or effecters.

One of the well-documented examples of K63-polyubiquitination in signal transduction has been the activation of IKK complex (IKKα/IKKβ/NEMO), which functions as the kinase to phosphorylate IκB under multiple stimulations, including IL1β. Following years of intensive studies with cell biology and biochemistry, it is now accepted that upon binding of the ligand such as IL1β to its receptor, the adaptor proteins MyD88 and IRAK1 are recruited and further recruit and activate downstream ubiquitin-ligase TRAF6. Working in an enzymatic cascade with E2 complex of Ubc13/Uev1a, TRAF6 catalyzes the formation of K63-linked ubiquitin-chain to the target proteins including itself.

K63-polyubiquitin chain then functions as a scaffold to activate TAK1/TAB2/TAB3 and bring the two kinase complexes of TAK1/TAB2/TAB3 and IKKα/IKKβ/NEMO into adjacency through ubiquitin binding domains on TAB2/TAB3 and NEMO, which results in phosphorylation and activation of IKK complex by TAK1 (Chen, 2005)). Other examples of K63-polyubiquitination involved in signaling events include K63-polyubiquitinated Histones in DNA repair (Doil et al., 2009).

The finding of MAVS-mediated IRF3 activation through K63-linked polyubiquitination not only provides the mechanism for TBK1 complex (TBK1/TANK/NEMO) activation, but also suggests a broader signaling role of K63-linked ubiquitin-chains. Furthermore, an intriguing question aroused by this study has been whether activation of IRFs through other PAMP-receptors might also exploit the same mechanism involving K63-polyubiquitination. For instance, although it is generally believed that TLRs and cytosolic microbial DNA receptor(s) activate downstream IRFs also through TBK1 and/or IKKε or Ikkα, the molecular mechanism is largely unknown (Honda et al., 2006; Honda and Taniguchi, 2006), Given the reports that NEMO is required for TLR3-mediated IRF3 activation (Zhao et al., 2007), and more interestingly, the E3 ligases TRAF3

and TRAF6 are involved in signaling from multiple TLRs to activate NF-κB or IRFs, it is conceivable that K63-linked ubiquitination could also play a key role in these processes. A similar strategy employing biochemical assay and RNAi-knockdown cells will be helpful to reveal the answers.

Similarity between the mechanisms of activating IKK complex and TBK1 complex made it tempting to speculate that a common theme of K63-linked ubiquitin-chain as a scaffold for adaptors could be underlying other regulatory events, e.g., viral activation of RIG-I by TRIM25. Currently, several proteins have been shown to exert ubiquitin-binding capability, particularly with specificity to K63-linked conjugation, i.e., TAB2 and NEMO (Ea et al., 2006; Kanayama et al., 2004; Wu et al., 2006). And a more comprehensive proteomic characterization of K63-polyubiquitination adaptors will likely elucidate the scope of this specific form of polyubiquitination as signaling component in mammalian cells.

The sharing of K63-linked ubiquitin-chains between distinct signaling pathways has posed a critical question of whether one adaptor could bind the same ubiquitin-chain to activate divergent downstream signals, e.g., whether NEMO could mediate the activation of TBK1 complex and IKK complex on the same ubiquitin-chain. Activation of one particular signaling pathway but not

others could possibly rely on the proteins targeted for ubiquitin conjugation, which would help to provide a multivalent binding site for specific adaptors. Conversely, the utilization of the same ubiquitin-chain by distinct adaptors might serve as a convergent point for signaling cross-talk between otherwise separated pathways.

Specificity of Ubiquitin-Conjugating Enzyme E2

Ubiquitin-conjugating enzyme E2 plays an indispensable role in ubiquitination reaction cycle (Fig. 3A). In addition to a conserved core domain for catalytic activity, some E2s have extensions on either N-terminal or C-terminal regions, which in some cases mediate localization and also protein interactions for determining substrate specificity (Plafker et al., 2004; Summers et al., 2008). In fact, four classes of E2 enzymes have been defined according to the composition of extensions, with Class I only containing core domain, Class II containing an additional C-terminal extension, Class III containing an additional N-terminal extension, and Class IV having extensions on both termini.

Ubc13 has been a unique member among E2 family, in that it exists in a tight complex with a regulatory subunit Uev1a. Moreover, as a Class I E2 enzyme,

Ubc13/Uev1a complex has been well characterized for its strict specificity to synthesize K63-linked ubiquitin-chains (Hofmann and Pickart, 1999). Such specificity for ubiquitin linkage has been explained from structural studies on Ubc13/Mms2, the Ubc13/Uev1a ortholog in *Saccharomyces cerevisiae*, in which Mms2 positions the acceptor ubiquitin in such a specific way that only K63-linkage can be formed due to physical hindrance on other Lys-residues (Eddins et al., 2006; VanDemark et al., 2001). Besides Ubc13/Uev1a, another E2 reported to be able to catalyze K63-linked ubiquitin-chain is UbcH7 (Geetha et al., 2005), but definitive evidence remains lacking.

In contrast to strict specificity to K63-polyubiquitination of Ubc13/Uev1a, Ubc5 has been known to synthesize ubiquitin chains with various linkages, i.e., K48-, K63- or even K11-linked ubiquitin-chain. Based on solved structures of Ubc5 in complex with ubiquitin, no obvious features are apparent to determine the linkage specificity (Houben et al., 2004). Interestingly, non-covalent *in trans* interaction between intermediate forms of Ubc5~Ub exists (Brzovic et al., 2006), which might allow Ubc5~Ub to assemble into large polymeric complex and thus synthesize more diversified ubiquitin-chains than other E2s.

Given its "promiscuous" specificity to ubiquitin linkage, it has been a

surprise that Ubc5 but not Ubc13/Uev1a was required in K63-polyubiquitination -mediated IRF3 activation (Fig. 9). One possibility was that, similar to Ubc13/Uev1a, an unknown regulatory subunit of Ubc5 might regulate preference to K63-linkage in cells. Although the failure to co-purify such a regulatory protein in my fractionation procedures seemed to argue against the idea, it was not ruled out that other crude fraction (P5 or Q-B) might provide such a putative component. An improved assay system solely based on recombinant proteins will help to resolve the issue. Alternatively, another explanation to K63-linkage could probably rely on ubiquitin-ligase E3(s) involved in the process. Previous studies have demonstrated that Ubc5 could mediate synthesis of various forms of ubiquitin-chain with different E3s, e.g., Ubc5 catalyzes K63-polyubiquitination with Nedd4, whereas K48-polyubiquitination is formed with E6AP (Kim et al., 2007). Therefore, identification of functional E3(s) involved in the process is a critical step in this line of research (see below).

Ubiquitin-Ligase E3(s) Functioning in Viral Activation of IRF3

A major unanswered question remained in current study is the lack of definitive proof to the identity of ubiquitin-ligase(s) and target(s) in signaling

cascade to activate IRF3. Among several E3 enzymes implied in the pathway, TRAF3 appeared to be the most promising candidate, since a modest but consistent defect in IFNβ production was observed in TRAF3-deficient MEF cells upon viral infection (Fig. 19A). Based on the observation that TRAF3 got auto-ubiquitinated upon stimulation, it is reasonable to speculate that TRAF3 could serve as both E3 and target in the signaling event.

However, viral activation of IRF3 was only mildly affected in the absence of TRAF3 (Fig. 19B), and virtually no defect was observed with the loss of other candidate TRAF proteins (Fig. 18). One possibility was a functional redundancy existing among members of TRAF and/or TRIM family in IRF3 pathway, which could help to largely compensate the function of each other. Such a redundancy would also readily explain the failure to uncover a specific E3 through siRNA-knockdown screening. To overcome the difficulty, a pure biochemical assay based on recombinant proteins will again be a reasonable option, through testing the ability of each candidate E3 to activate IRF3 *in vitro*. Finally, a definitive answer to the identity of E3(s) and ubiquitin targets will rely on identification of the components contributed by Q-B fraction in the *in vitro* assay.

CHAPTER IV: EXPERIMENTAL PROCEDURES

Materials and General Methods

[^{35}S]Methionine was purchased from PerkinElmer. Nickel-affinity resin was from QIAGEN, and all other chromatography columns were from GE Healthcare. Methylated-ubiquitin was from Boston Biochem. Anti-Flag M2 affinity gel, Flag peptide, solvents, and other chemicals were from Sigma unless otherwise specified.

Tetracycline was added to culture medium at a final concentration of 1 μg/ml. Sendai virus (Cantell strain, Charles River Laboratories) was used at a final titration of 100 hemagglutinating(HA)-units/ml. VSV(M51)-GFP virus was kindly provided by Dr. John Bell (University of Ottawa), and propagated in Vero cells as described (Stojdl et al., 2003).

Native PAGE was carried out in 4 degree. Briefly, cathode buffer contained 25mM Tris, 192mM Glycine. Anode buffer contained 25mM Tris, 192mM Glycine and 0.4% NaDOC. The PAGE was pre-run at 200V for 60 minutes and proteins were resolved at 200V for 60 minutes.

Antibodies

Antibody against TBK1 was from Cell signaling; ubiquitin, NEMO, TRAF3, and human-IRF3 from Santa Cruz Biotech; mouse-IRF3 from Zymed; monoclonal anti-HA from Covance; polyclonal anti-HA, and monoclonal anti-Flag from Sigma. Antibody against human Ubc5 was kindly provided by Dr. Allan Weisssman (National Institutes of Health). Antibodies against MAVS and RIG-I were generated in the laboratory as previously reported (Seth et al., 2005). Goat anti-rabbit IgG or anti-mouse IgG conjugated to alkaline phosphatase were from Promega. Standard methods of molecular biology were followed unless otherwise specified.

Immunoblot Analysis

Cells were homogenized in buffer containing 20 mM Tris-Cl (pH 7.5), 150 mM NaCl, 10% (v/v) glycerol, 1 mM dithiothreitol (DTT), 1% (w/v) TritonX-100, 20 mM β-glycerol phosphate,1 mM Na_3VO_4, 0.1 mM NaF, 0.1 mM PMSF, and protease inhibitors cocktail (Roche). After incubation on ice for 10 minutes, lysate was centrifuged at 20,000 *g* for 15 minutes. An aliquot of the supernatant containing 20 μg of total proteins was subjected to gel electrophoresis, followed

by immunoblot analysis with antibodies as indicated in figure legends.

Calcium Phosphate Precipitation Method

HEK293T cells were set up in 12-well plates at day 0 unless otherwise specified in figure legends. cDNAs or siRNAs were diluted in 37.5 μl H_2O and mixed with 12.5 μl of 1M $CaCl_2$. 50 μl of 2×HBS buffer containing 50mM HEPES (pH 7.05), 10 mM KCl, 12 mM Dextrose, 280 mM NaCl, and 1.5 mM Na_2HPO_4 was added to the mixture, and the mixture was then added to cells drop-wise immediately following brief vortex.

Cell Culture, Transfection, and Luciferase-Reporter Assay

All cells were cultured in monolayer at 37°C in an atmosphere of 5% (v/v) CO_2. HEK293T and HEK293T-MAVS (HEK293T cell line stably transfected with Flag-MAVS) were cultured in DMEM with 10% (v/v) cosmic calf serum (Hyclone), 100 U/ml penicillin and 100 μg/ml streptomycin. Human osteosarcoma U2OS cells were cultured in DMEM with 10% (v/v) FBS (tetracycline-free, Invitrogen), 100 U/ml penicillin and 100 μg/ml streptomycin. All MEF cells were cultured in DMEM with 10% (v/v) FBS, 100 U/ml penicillin

and 100 μg/ml streptomycin.

For RNAi-knockdown in HEK293T cells, cells were set up in 12-well plates on day 0. On day 1, siRNA were transfected in duplicate at a final concentration of 20 nM using calcium phosphate precipitation method. On day 2, siRNA was transfected a second time with 50 ng of luciferase-reporter driven by either interferon-stimulated response element (ISRE) or interferon-β promoter (IFNβ). 100 ng of pCMV-LacZ was included in each well as an internal control of transfection efficiency. On day 4, cells were infected with SeV for 16 hours before luciferase and β-galactosidase activities were measured. siRNA oligo (sense-strand) sequences were: GFP, ACUUGUACAGCUCGUCCAUTT; Ubc5, CAGUAAUGGCAGCAUUUGUTT; MAVS, CCACCUUGAUGCCUGUGAATT; RIG-I, CGAUUCCAUCACUAUCCAUTT; and TBK1, UCAAGAACUUAUCUACGAATT.

For transient overexpression in HEK293T cells, cells were set up in 12-well plates on day 0 unless otherwise specified in figure legends. On day 1, expression plasmids were transfected in duplicate at 0.5 μg per well with 50 ng of ISRE- or IFNβ-luciferase using calcium phosphate precipitation method. 100 ng of pCMV-LacZ was included in each well as an internal control of transfection

efficiency. On day 2, cells were infected with SeV for 16 hours before luciferase and β-galactosidase activities were measured.

For luciferase-reporter assays in NEMO-deficient MEF cells, cells were set up in 12-well plates on day 0. On day 1, 20 ng of expression vectors for indicated versions of NEMO were transfected together with 250 ng of ISRE-luciferase in duplicate using Lipofectamine 2000 (Invitrogen) following manufacturer's instruction. 250 ng of pCMV-(Renilla Luciferase) was included in each well as an internal control of transfection efficiency. On day 2, VSV(M51)-GFP was added to each well at an MOI of 1, and luciferase activities were measured 14-hour post-infection.

For luciferase reporter assays in U2OS cells, cells were set up in 6-well plates on day 0. On day 1, tetracycline was added at final concentration of 1 μg/ml. Expression vector was transfected on day 6 at 0.15 μg per well with 100 ng of ISRE-luciferase in duplicate using Lipofectamine LTX (Invitrogen) following manufacturer's instruction. 500 ng of pCMV-(Renilla Luciferase) was included in each well as an internal control of transfection efficiency, and luciferase activities were measured on day 8.

ELISA Measurement of Interferon-β

For measurement of human interferon-β produced in U2OS cells, cells were set up in 6-well plates on day 0, and treated with mock or tetracycline on day 1 as indicated. Cells were infected on day 6 with Sendai virus, and medium from individual condition was harvested 16-hour post-infection for analysis with Human IFN-Beta ELISA Kit (PBL Biomedical Laboratories).

For measurement of mouse interferon-β produced in MEF cells, cells were set up in 6-well plates on day 0, and infected on day 1 with Sendai virus for 16 hours or indicated times. Medium from individual condition was harvested for analysis using Mouse IFN-Beta ELISA Kit (PBL Biomedical Laboratories).

Real-Time PCR

Total RNA from HEK293T cells was extracted using TRIZOL (Invitrogen). 2 μg of total RNA was reverse-transcribed into cDNA using random hexamer (Applied Biosystems). Real-time PCR was carried out using IQ SYBR Green Kit (Bio-Rad) with primers for GAPDH (5'-ATGACATCAAGAAGGTGGTG-3' and 5'-CATACCAGGAAATGAGCTTG-3'), and for mouse IFNβ (5'-AGGACAGG ATGAACTTTGAC-3' and 5'-TGATAGACATTAGCCAGGAG-3').

Immuno-precipitation

HEK293T cells were set up in 100-mm dish on day 0. On day 1, each dish of cells were transfected with 2 μg of pcDNA3-His-TANK-HA, 3 μg of pcDNA3-Flag-NEMO or indicated version of mutants, and 3 μg of pcDNA3-Flag-TBK1 by calcium phosphate precipitation method. Cells were harvested on day 3, and lysed in buffer containing 20 mM Tris-Cl (pH 7.5), 150 mM NaCl, 10% (v/v) glycerol, 1 mM dithiothreitol, 1% (w/v) TritonX-100, 20 mM β-glycerol phosphate, 1 mM Na_3VO_4, 0.1 mM NaF, 0.1 mM PMSF, and EDTA-free protease inhibitors cocktail. After incubation on ice for 10 minutes, lysate was centrifuged at 20,000 *g* for 15 minutes. Supernatant was incubated with rat monoclonal anti-HA agarose (Roche) at 4^{o}C for 5 hours. After washing the beads four times with the same buffer, bound proteins were eluted by boiling the beads in loading buffer (50 mM Tris-Cl at pH 6.8, 1% (w/v) SDS, 50 mM DTT, and 5% (v/v) glycerol).

Purification of Recombinant NEMO from Culture Cells

Expression constructs for various versions of human NEMO were prepared by inserting DNA segments encoding NEMO WT (aa1-419), ΔKBD (aa86-419),

ΔZF (aa1-365), and ΔLZZF (aa1-302) into pcDNA3 vector driven by cytomegalovirus (CMV) promoter-enhancer. An N-terminal Flag-tag was included to facilitate protein purification and detection. Mutant versions of Y308S and ΔZF-Y308S were generated by QuikChange Site-Directed Mutagenesis Kit (Stratagene) from constructs of NEMO WT and ΔZF, respectively.

For purification of recombinant NEMO proteins, each expression construct was transfected into HEK293T cells. Cells were harvested 48-hour post-transfection, and lysed in buffer containing 20 mM Tris-Cl (pH 7.5), 150 mM NaCl, 10% (v/v) glycerol, 1 mM dithiothreitol, 1% (w/v) TritonX-100, 0.1 mM PMSF, and EDTA-free protease inhibitors cocktail. After incubation on ice for 10 minutes, lysate was centrifuged at 20,000 *g* for 15 minutes. Supernatant was incubated with anti-Flag M2 agarose at 4^{o}C for 4 hours. After washing the beads three times with the same buffer, NEMO proteins were eluted with 200 μg/ml Flag peptide in elution buffer containing 20 mM Tris-Cl (pH7.5), 100 mM NaCl, 10% (v/v) glycerol, 20 mM β-glycerol phosphate and 1 mM Na_3VO_4. NEMO proteins were concentrated, and buffer changed to 20 mM HEPES-KOH (pH 7.0), 10% (v/v) glycerol and 0.02% CHAPS with 10KD concentrator (Millipore).

Purification of Recombinant Proteins from Bacteria

Ubiquitin and mutant versions were expressed in a modified *E. coli* strain BL21(DE3)-pJY2 to prevent mis-incorporation of Lys residues. Bacteria was lysed in buffer containing 50mM HEPES-KOH (pH 6.5), 0.1 mM PMSF, EDTA-free Protease inhibitor, 1mM β-mercaptoethanol followed by sonication for 3 minutes. Supernatant following 100,000g centrifuge for 30 minutes was loaded onto Q-Sepharose column equilibrated with 20 mM HEPES-KOH (pH6.7), 10% (v/v) Glycerol and 0.02% CHAPS. Flow-through was collected, and added buffer HEPES-KOH (pH 7.5) to 20 mM and loaded to SP-Sepharose column equilibrated with 20 mM HEPES-KOH (pH7.0), 10% (v/v) Glycerol and 0.02% CHAPS. Flow-through of SP-Sepharose was further fractionated on Superdex-75 in 20 mM HEPES-KOH (pH7.0), 10% (v/v) Glycerol and 0.02% CHAPS. Fractions with ubiquitin proteins were pooled, aliquoted and stored at -80^{o}C.

His_6-Ubc13 and His_6-Uev1A were purified from *E. coli* through Nickel-affinity chromatography. Human E2-25K, Ubc3, Ubc5a, Ubc5b, Ubc5c, Ubc5c (C85A), Ubc7, NEMO and NEMO-ZF(aa360-419) were all expressed in *E. coli* as GST-fusion proteins, and purified through glutathione-affinity chromatography. For GST-E2s, after releasing GST by thrombin cleavage,

proteins were further purified on either SP-Sepharose column (Ubc5a, Ubc5b, Ubc5c, Ubc5c-C85A and Ubc7) containing 20 mM HEPES-KOH (pH7.0), 10% Glycero and 0.02% CHAPS, or Q-Sepharose column (E2-25K and Ubc3) in buffer containing 20 mM Tris-Cl (pH 7.5), 10% (v/v) Glycerol and 0.02% CHAPS.

Purification of Recombinant Protein from Insect Cells

For baculoviral expression in Sf9 insect cells, cDNA encoding human TRAF3 with an N-terminal His_8-tag was cloned into pFastBac1, and human E1 and human TRAF6 into pFastBac HT-A (Invitrogen). Baculovirus was generated followed manufacturer's instructions, and the titer of P3 virus was estimated to be 1×10^8 pfu/ml. Sf9 insect cells were cultured in Sf-900 II SFM, and set up in suspension on day 0. On day 1, cells were infected at a density of 1×10^6 cells per ml with baculovirus (MOI ranging from 2 to 4). Cells were harvested 48-hour post-infection, washed once with PBS, and stored at -80^{o}C.

Cells were disrupted on ice with a Dounce homogenizer by 40 strokes in Buffer A (50 mM Tris-Cl at pH 7.5, 150 mM NaCl, 1 mM β-mercaptoethanol, and protease inhibitors cocktail). Following a centrifugation at 1,000 *g* for 5 min, a

final concentration of 0.5% (w/v) TritonX-100 was added to the supernatant, after which the mixture was further centrifuged at 100,000 *g* for 1 hour. The supernatant was loaded onto nickel-affinity column, and protein was eluted in Buffer A containing 250 mM imidazole. After overnight dialysis against buffer containing 20 mM HEPES-KOH (pH 7.5), 10% (v/v) glycerol, 0.1mM DTT and 0.1 PMSF at 4^{o}C, protein was aliquoted and stored at -80^{o}C.

In Vitro Assay for IRF3 Activation

All assay procedures were carried out at 4°C unless otherwise specified. After homogenization of culture cells in hypotonic buffer (10 mM Tris-Cl at pH 7.5, 10 mM KCl, 0.5 mM EGTA, 1.5 mM $MgCl_2$, and EDTA-free protease inhibitor cocktail), homogenates were centrifuged at 1,000 *g* for 5 minutes to pellet nuclei and unbroken cells (P1). The supernatant (S1) was subjected to centrifugation at 5,000 *g* for 10 minutes to separate crude mitochondrial pellet from cytosolic supernatant (S5). Mitochondrial pellet was washed once with MRB buffer (20 mM HEPES-KOH at pH 7.4, 10% (v/v) glycerol, 0.5 mM EGTA, and EDTA-free protease inhibitor cocktail), and re-suspended in MRBC buffer (MRB buffer containing 1% (w/v) CHAPS and EDTA-free protease inhibitor).

After a centrifugation at 10,000 *g* for 15 minutes, the supernatant was hereafter designated as P5 in the assays. For preparation of viral-activated P5, cells were infected with Sendai virus for 16 hours before the fractionation procedure. Most of the assays were carried out using P5 and S5, but for biochemical fractionation, S5 was further centrifuged at 100,000 *g* for 1 hour to obtain cytosolic extract (S100).

^{35}S-IRF3 was *in vitro* synthesized with pcDNA3-Flag-IRF3 as template using TNT Coupled Reticulocyte Lysate Transcription/Translation Kit (Promega). For each 10-µl reaction, 4 µg of P5, 30 to 40 µg of cytosolic fraction (S5 or S100), and 0.5 µl of ^{35}S-IRF3 were mixed in buffer containing 20 mM HEPES-KOH (pH 7.0), 2 mM ATP, and 5 mM $MgCl_2$. After incubation at 30°C for 1 hour, the samples were subjected to native PAGE, and dimerization of ^{35}S-IRF3 was visualized by autoradiography using PhosphorImager (GE Healthcare).

Biochemical Fractionation of Cytosolic Extract

HeLa cytosolic extract (S100) was prepared as described above from 50 liter of cells purchased from National Cell Culture Center. S100 was loaded onto 60 ml Q-Sepharose column equilibrated with buffer Q-A (20 mM Tris-Cl at pH 7.5, 10%

(v/v) glycerol, and 0.02% (w/v) CHAPS), and flow-through was precipitated with 40% to 80% (w/v) of ammonium sulfate. After centrifugation at 10,000 *g* for 30 min, precipitates were re-suspended in buffer SP-A (20 mM HEPES-KOH at pH 7.0, 10% (v/v) glycerol, and 0.02% (w/v) CHAPS), and subjected to dialysis against buffer SP-A. The sample was further fractionated on 1 ml Heparin-Sepharose column with a linear gradient of NaCl (0 mM to 300 mM) in buffer SP-A, and active fractions eluted around 150 mM NaCl were pooled. After buffer content was changed to SP-A by repeated concentrating, proteins was separated on 1 ml SP-Sepharose column with a linear gradient of NaCl (0 mM to 300 mM) in buffer SP-A. Active fractions eluted around 150 mM NaCl were concentrated, and fractionated onto Superdex-75 column. *In vitro* assay for IRF3 activation was performed following each step of chromatography. 1% of Superdex-75 fractions were subjected to SDS-PAGE, and proteins were visualized by silver-staining. The protein band correlating with IRF3-activating activity was analyzed by tandem mass spectrometry.

Tetracycline-Inducible Expression of shRNA and Transgene

U2OS cells stably expressing tetracycline-repressor were chosen as the

parental cell line. Tetracycline-inducible knockdown constructs and rescue constructs were generated as following.

Briefly, pSuperior and pBluescript vectors were employed to obtain tandem cassettes of shRNA driven by H1-promoter, and pHygro and pPur vectors were used to generate final tetracycline-inducible knockdown constructs. Four tandem cassettes of Ubc5 shRNA-1 (CCACCTAAGGTTGCATTTA) and four tandem cassettes of Ubc5 shRNA-2 (CAGTAATGGCAGCATTTGT) were inserted together into pHygro vector to make the knockdown construct Ubc5b/c(KD). Six tandem cassettes of shRNA against UBA52 and UBC (ACACCATTGAGAATGT CAA) and four tandem cassettes of shRNA against RPS27 and UBB (AGGCCAAGATCCAGGATAA) were inserted together into pPur vector to make the knockdown construct Ub(KD). Plasmids were transfected by Lipofectamine 2000 (Invitrogen) into U2OS cells, and single colonies were selected in 400 μg/ml and further maintained in 200 μg/ml hygromycin (Ubc5b/c(KD)), or selected in 2 μg/ml and further maintained in 1 μg/ml puromycin (Ub(KD)).

For rescue experiments, the expression constructs were generated on modified pcDNA3 vector with CMV-promoter substituted by H1-promoter (pcDNA3-H1). Wildtype or C85A-mutant cDNAs of Ubc5c with the following

mutations were cloned into pcDNA3-H1 to render RNAi-resistant forms of Flag-Ubc5c: CC*T*CC*A*AAA*A*GT*A*GC*T*TT*C*A and *T*AG*C*AA*C*GG*G*AG*T*AT*C*TG*C* (mutations in italics). Similarly, the following mutations were introduced into UBA52 (A*T*AC*A*AT*C*GA*A*AAA*C*GTCAA, mutations in italics), and RPS27 (A*A*GC*T*AA*A*AAT*T*CAGGA*C*AA, mutations in italics) to render RNAi-resistant forms of ubiquitin. A HA-tag was added to the N-terminus of RPS27, and for K63R ubiquitin, the corresponding mutation was also introduced into UBA52 and RPS27. RNAi-resistant versions of UBA52 and RPS27 were then linked through an IRES (Internal Ribosome Entry Site) and cloned into pcDNA3-H1 (Fig. 5C). The resulting rescue constructs were transfected into either Ubc5b/c(KD) or Ub(KD) cells, and rescue colonies were selected in 800 μg/ml and further maintained in 400 μg/ml G418, in addition to the original presence of hygromycin or puromycin, respectively.

For analysis of IRF3 dimerization, Ubc5b/c- or Ub-knockdown and rescue cells were set up in 6-well plates on day 0 and treated with mock or tetracycline on day 1. The cells were infected on day 4 (Ub) or day 6 (Ubc5b/c) with Sendai virus for indicated times before the cell lysates were prepared for native PAGE as described above.

Ubiquitin-Chain Binding Assay

K63-linked ubiquitin-chains was synthesized at 30°C for 2 hours in 100-µl reaction containing 0.5 µg His_6-E1, 2 µg His_6-Ubc13/Uev1A, 3 µg His_6-TRAF6 and 100 µg HA-Ubiquitin in the presence of 2 mM ATP. 20 pmol of Flag-NEMO or indicated mutant versions was incubated with K63-linked ubiquitin-chain at room temperature for 30 minutes in 200-µl mixture containing 20 mM HEPES-KOH (pH 7.0), 10% (v/v) glycerol, 50 mM NaCl, and 0.1% (w/v) NP-40. After immune-precipitation of Flag-tagged NEMO proteins with anti-Flag M2 beads, interaction of ubiquitin-chain was examined by immunoblot analysis with anti-HA antibody.

RNAi-Knockdown Screening of E3 Library

HEK293T cells stably transfected with IFNβ-Luciferase and pCMV-(Renilla Luciferase) (constructed by Dr. Yu-Hsin Chiu) were set up in 96-well plates on day 0. Four pairs of siRNA targeting each predicted human E3 (QIAGEN) was pooled, and transfected at a final concentration of 20 nM using calcium phosphate precipitation on day 1. Cells were infected on day 3 with Sendai virus for 16 hours before luciferase activities were measured on day 4.

For epistasis studies, HEK293T cells were set up in 24-well plates on day 0. Four pairs of siRNA targeting each predicted human E3 (QIAGEN) was pooled, and transfected at a final concentration of 20 nM using calcium phosphate precipitation method on day 1. 0.5 ug of expression vectors for RIG-I-N or TBK1 were transfected at day 2 together with siRNA and ISRE-Luciferase (RIG-I-N) or IFNβ-Luciferas (TBK-1) and pCMV-(Renilla Luciferase) reporters using calcium phosphate precipitation method. Luciferase activities were measured on day 4.

CHAPTER V: REFERENCES

Adhikari, A., Xu, M., and Chen, Z. J. (2007). Ubiquitin-mediated activation of TAK1 and IKK. Oncogene *26*, 3214-3226.

Alexopoulou, L., Holt, A. C., Medzhitov, R., and Flavell, R. A. (2001). Recognition of double-stranded RNA and activation of NF-kappaB by Toll-like receptor 3. Nature *413*, 732-738.

Baril, M., Racine, M. E., Penin, F., and Lamarre, D. (2009). MAVS dimer is a crucial signaling component of innate immunity and the target of hepatitis C virus NS3/4A protease. J Virol *83*, 1299-1311.

Beutler, B., Eidenschenk, C., Crozat, K., Imler, J. L., Takeuchi, O., Hoffmann, J. A., and Akira, S. (2007). Genetic analysis of resistance to viral infection. Nat Rev Immunol *7*, 753-766.

Beutler, B., Jiang, Z., Georgel, P., Crozat, K., Croker, B., Rutschmann, S., Du, X., and Hoebe, K. (2006). Genetic analysis of host resistance: Toll-like receptor signaling and immunity at large. Annu Rev Immunol *24*, 353-389.

Bode, J. G., Brenndorfer, E. D., and Haussinger, D. (2007). Subversion of innate host antiviral strategies by the hepatitis C virus. Arch Biochem Biophys *462*, 254-265.

Bowie, A. G., and Unterholzner, L. (2008). Viral evasion and subversion of pattern-recognition receptor signalling. Nat Rev Immunol *8*, 911-922.

Bradley, J. R., and Pober, J. S. (2001). Tumor necrosis factor receptor-associated factors (TRAFs). Oncogene *20*, 6482-6491.

Brzovic, P. S., Lissounov, A., Christensen, D. E., Hoyt, D. W., and Klevit, R. E. (2006). A UbcH5/ubiquitin noncovalent complex is required for processive BRCA1-directed ubiquitination. Mol Cell *21*, 873-880.

Chariot, A., Leonardi, A., Muller, J., Bonif, M., Brown, K., and Siebenlist, U. (2002). Association of the adaptor TANK with the I kappa B kinase (IKK) regulator NEMO connects IKK complexes with IKK epsilon and TBK1 kinases. J Biol Chem *277*, 37029-37036.

Chen, Z. J. (2005). Ubiquitin signalling in the NF-kappaB pathway. Nat Cell Biol *7*, 758-765.

Chen, Z. J., and Sun, L. J. (2009). Nonproteolytic functions of ubiquitin in cell signaling. Mol Cell *33*, 275-286.

Choe, J., Kelker, M. S., and Wilson, I. A. (2005). Crystal structure of human

toll-like receptor 3 (TLR3) ectodomain. Science *309*, 581-585.
Ciechanover, A., and Ben-Saadon, R. (2004). N-terminal ubiquitination: more protein substrates join in. Trends Cell Biol *14*, 103-106.
Clark, R., and Kupper, T. (2005). Old meets new: the interaction between innate and adaptive immunity. J Invest Dermatol *125*, 629-637.
Cordier, F., Grubisha, O., Traincard, F., Veron, M., Delepierre, M., and Agou, F. (2009). The zinc finger of NEMO is a functional ubiquitin-binding domain. J Biol Chem *284*, 2902-2907.
Cui, S., Eisenacher, K., Kirchhofer, A., Brzozka, K., Lammens, A., Lammens, K., Fujita, T., Conzelmann, K. K., Krug, A., and Hopfner, K. P. (2008). The C-terminal regulatory domain is the RNA 5'-triphosphate sensor of RIG-I. Mol Cell *29*, 169-179.
Doil, C., Mailand, N., Bekker-Jensen, S., Menard, P., Larsen, D. H., Pepperkok, R., Ellenberg, J., Panier, S., Durocher, D., Bartek, J., *et al.* (2009). RNF168 binds and amplifies ubiquitin conjugates on damaged chromosomes to allow accumulation of repair proteins. Cell *136*, 435-446.
Ea, C. K., Deng, L., Xia, Z. P., Pineda, G., and Chen, Z. J. (2006). Activation of IKK by TNFalpha requires site-specific ubiquitination of RIP1 and polyubiquitin binding by NEMO. Mol Cell *22*, 245-257.
Eddins, M. J., Carlile, C. M., Gomez, K. M., Pickart, C. M., and Wolberger, C. (2006). Mms2-Ubc13 covalently bound to ubiquitin reveals the structural basis of linkage-specific polyubiquitin chain formation. Nat Struct Mol Biol *13*, 915-920.
Ferrandon, D., Imler, J. L., Hetru, C., and Hoffmann, J. A. (2007). The Drosophila systemic immune response: sensing and signalling during bacterial and fungal infections. Nat Rev Immunol *7*, 862-874.
Fitzgerald, K. A., McWhirter, S. M., Faia, K. L., Rowe, D. C., Latz, E., Golenbock, D. T., Coyle, A. J., Liao, S. M., and Maniatis, T. (2003). IKKepsilon and TBK1 are essential components of the IRF3 signaling pathway. Nat Immunol *4*, 491-496.
Fredericksen, B. L., Keller, B. C., Fornek, J., Katze, M. G., and Gale, M., Jr. (2008). Establishment and maintenance of the innate antiviral response to West Nile Virus involves both RIG-I and MDA5 signaling through IPS-1. J Virol *82*, 609-616.
Friedman, C. S., O'Donnell, M. A., Legarda-Addison, D., Ng, A., Cardenas, W. B., Yount, J. S., Moran, T. M., Basler, C. F., Komuro, A., Horvath, C. M.,

et al. (2008). The tumour suppressor CYLD is a negative regulator of RIG-I-mediated antiviral response. EMBO Rep *9*, 930-936.

Fritz, J. H., Ferrero, R. L., Philpott, D. J., and Girardin, S. E. (2006). Nod-like proteins in immunity, inflammation and disease. Nat Immunol *7*, 1250-1257.

Gack, M. U., Shin, Y. C., Joo, C. H., Urano, T., Liang, C., Sun, L., Takeuchi, O., Akira, S., Chen, Z., Inoue, S., and Jung, J. U. (2007). TRIM25 RING-finger E3 ubiquitin ligase is essential for RIG-I-mediated antiviral activity. Nature *446*, 916-920.

Gale, M., Jr., and Foy, E. M. (2005). Evasion of intracellular host defence by hepatitis C virus. Nature *436*, 939-945.

Geetha, T., Jiang, J., and Wooten, M. W. (2005). Lysine 63 polyubiquitination of the nerve growth factor receptor TrkA directs internalization and signaling. Mol Cell *20*, 301-312.

Gitlin, L., Barchet, W., Gilfillan, S., Cella, M., Beutler, B., Flavell, R. A., Diamond, M. S., and Colonna, M. (2006). Essential role of mda-5 in type I IFN responses to polyriboinosinic:polyribocytidylic acid and encephalomyocarditis picornavirus. Proc Natl Acad Sci U S A *103*, 8459-8464.

Grandvaux, N., tenOever, B. R., Servant, M. J., and Hiscott, J. (2002). The interferon antiviral response: from viral invasion to evasion. Curr Opin Infect Dis *15*, 259-267.

Guo, B., and Cheng, G. (2007). Modulation of the interferon antiviral response by the TBK1/IKKi adaptor protein TANK. J Biol Chem *282*, 11817-11826.

Hacker, H., Redecke, V., Blagoev, B., Kratchmarova, I., Hsu, L. C., Wang, G. G., Kamps, M. P., Raz, E., Wagner, H., Hacker, G., *et al.* (2006). Specificity in Toll-like receptor signalling through distinct effector functions of TRAF3 and TRAF6. Nature *439*, 204-207.

Hale, B. G., Randall, R. E., Ortin, J., and Jackson, D. (2008). The multifunctional NS1 protein of influenza A viruses. J Gen Virol *89*, 2359-2376.

Hicke, L., and Dunn, R. (2003). Regulation of membrane protein transport by ubiquitin and ubiquitin-binding proteins. Annu Rev Cell Dev Biol *19*, 141-172.

Hofmann, R. M., and Pickart, C. M. (1999). Noncanonical MMS2-encoded ubiquitin-conjugating enzyme functions in assembly of novel polyubiquitin chains for DNA repair. Cell *96*, 645-653.

Honda, K., Takaoka, A., and Taniguchi, T. (2006). Type I interferon [corrected] gene induction by the interferon regulatory factor family of transcription factors.

Immunity *25*, 349-360.
Honda, K., and Taniguchi, T. (2006). IRFs: master regulators of signalling by Toll-like receptors and cytosolic pattern-recognition receptors. Nat Rev Immunol *6*, 644-658.
Hornung, V., Ellegast, J., Kim, S., Brzozka, K., Jung, A., Kato, H., Poeck, H., Akira, S., Conzelmann, K. K., Schlee, M., *et al.* (2006). 5'-Triphosphate RNA is the ligand for RIG-I. Science *314*, 994-997.
Houben, K., Dominguez, C., van Schaik, F. M., Timmers, H. T., Bonvin, A. M., and Boelens, R. (2004). Solution structure of the ubiquitin-conjugating enzyme UbcH5B. J Mol Biol *344*, 513-526.
Isaacs, A., and Lindenmann, J. (1957). Virus interference. I. The interferon. Proc R Soc Lond B Biol Sci *147*, 258-267.
Isaacs, A., Lindenmann, J., and Valentine, R. C. (1957). Virus interference. II. Some properties of interferon. Proc R Soc Lond B Biol Sci *147*, 268-273.
Ishikawa, H., and Barber, G. N. (2008). STING is an endoplasmic reticulum adaptor that facilitates innate immune signalling. Nature *455*, 674-678.
Janeway, C. A., Jr., and Medzhitov, R. (2002). Innate immune recognition. Annu Rev Immunol *20*, 197-216.
Jensen, J. P., Bates, P. W., Yang, M., Vierstra, R. D., and Weissman, A. M. (1995). Identification of a family of closely related human ubiquitin conjugating enzymes. J Biol Chem *270*, 30408-30414.
Jin, M. S., and Lee, J. O. (2008). Structures of the toll-like receptor family and its ligand complexes. Immunity *29*, 182-191.
Kanayama, A., Seth, R. B., Sun, L., Ea, C. K., Hong, M., Shaito, A., Chiu, Y. H., Deng, L., and Chen, Z. J. (2004). TAB2 and TAB3 activate the NF-kappaB pathway through binding to polyubiquitin chains. Mol Cell *15*, 535-548.
Kang, D. C., Gopalkrishnan, R. V., Wu, Q., Jankowsky, E., Pyle, A. M., and Fisher, P. B. (2002). mda-5: An interferon-inducible putative RNA helicase with double-stranded RNA-dependent ATPase activity and melanoma growth-suppressive properties. Proc Natl Acad Sci U S A *99*, 637-642.
Kato, H., Takeuchi, O., Mikamo-Satoh, E., Hirai, R., Kawai, T., Matsushita, K., Hiiragi, A., Dermody, T. S., Fujita, T., and Akira, S. (2008). Length-dependent recognition of double-stranded ribonucleic acids by retinoic acid-inducible gene-I and melanoma differentiation-associated gene 5. J Exp Med *205*, 1601-1610.
Kato, H., Takeuchi, O., Sato, S., Yoneyama, M., Yamamoto, M., Matsui, K.,

Uematsu, S., Jung, A., Kawai, T., Ishii, K. J., *et al.* (2006). Differential roles of MDA5 and RIG-I helicases in the recognition of RNA viruses. Nature *441*, 101-105.

Katze, M. G., Fornek, J. L., Palermo, R. E., Walters, K. A., and Korth, M. J. (2008). Innate immune modulation by RNA viruses: emerging insights from functional genomics. Nat Rev Immunol *8*, 644-654.

Kawai, T., and Akira, S. (2008). Toll-like receptor and RIG-I-like receptor signaling. Ann N Y Acad Sci *1143*, 1-20.

Kawai, T., Takahashi, K., Sato, S., Coban, C., Kumar, H., Kato, H., Ishii, K. J., Takeuchi, O., and Akira, S. (2005). IPS-1, an adaptor triggering RIG-I- and Mda5-mediated type I interferon induction. Nat Immunol *6*, 981-988.

Kayagaki, N., Phung, Q., Chan, S., Chaudhari, R., Quan, C., O'Rourke, K. M., Eby, M., Pietras, E., Cheng, G., Bazan, J. F., *et al.* (2007). DUBA: a deubiquitinase that regulates type I interferon production. Science *318*, 1628-1632.

Kim, H. T., Kim, K. P., Lledias, F., Kisselev, A. F., Scaglione, K. M., Skowyra, D., Gygi, S. P., and Goldberg, A. L. (2007). Certain pairs of ubiquitin-conjugating enzymes (E2s) and ubiquitin-protein ligases (E3s) synthesize nondegradable forked ubiquitin chains containing all possible isopeptide linkages. J Biol Chem *282*, 17375-17386.

Kirkpatrick, D. S., Hathaway, N. A., Hanna, J., Elsasser, S., Rush, J., Finley, D., King, R. W., and Gygi, S. P. (2006). Quantitative analysis of in vitro ubiquitinated cyclin B1 reveals complex chain topology. Nat Cell Biol *8*, 700-710.

Kumar, H., Kawai, T., Kato, H., Sato, S., Takahashi, K., Coban, C., Yamamoto, M., Uematsu, S., Ishii, K. J., Takeuchi, O., and Akira, S. (2006). Essential role of IPS-1 in innate immune responses against RNA viruses. J Exp Med *203*, 1795-1803.

Lamarre, D., Anderson, P. C., Bailey, M., Beaulieu, P., Bolger, G., Bonneau, P., Bos, M., Cameron, D. R., Cartier, M., Cordingley, M. G., *et al.* (2003). An NS3 protease inhibitor with antiviral effects in humans infected with hepatitis C virus. Nature *426*, 186-189.

Le Bon, A., and Tough, D. F. (2002). Links between innate and adaptive immunity via type I interferon. Curr Opin Immunol *14*, 432-436.

Li, K., Foy, E., Ferreon, J. C., Nakamura, M., Ferreon, A. C., Ikeda, M., Ray, S. C., Gale, M., Jr., and Lemon, S. M. (2005a). Immune evasion by hepatitis C virus NS3/4A protease-mediated cleavage of the Toll-like receptor 3 adaptor

protein TRIF. Proc Natl Acad Sci U S A *102*, 2992-2997.
Li, X. D., Sun, L., Seth, R. B., Pineda, G., and Chen, Z. J. (2005b). Hepatitis C virus protease NS3/4A cleaves mitochondrial antiviral signaling protein off the mitochondria to evade innate immunity. Proc Natl Acad Sci U S A *102*, 17717-17722.
Lin, R., Lacoste, J., Nakhaei, P., Sun, Q., Yang, L., Paz, S., Wilkinson, P., Julkunen, I., Vitour, D., Meurs, E., and Hiscott, J. (2006). Dissociation of a MAVS/IPS-1/VISA/Cardif-IKKepsilon molecular complex from the mitochondrial outer membrane by hepatitis C virus NS3-4A proteolytic cleavage. J Virol *80*, 6072-6083.
Martinon, F., and Tschopp, J. (2004). Inflammatory caspases: linking an intracellular innate immune system to autoinflammatory diseases. Cell *117*, 561-574.
McWhirter, S. M., Fitzgerald, K. A., Rosains, J., Rowe, D. C., Golenbock, D. T., and Maniatis, T. (2004). IFN-regulatory factor 3-dependent gene expression is defective in Tbk1-deficient mouse embryonic fibroblasts. Proc Natl Acad Sci U S A *101*, 233-238.
Meylan, E., Curran, J., Hofmann, K., Moradpour, D., Binder, M., Bartenschlager, R., and Tschopp, J. (2005). Cardif is an adaptor protein in the RIG-I antiviral pathway and is targeted by hepatitis C virus. Nature *437*, 1167-1172.
Meylan, E., Tschopp, J., and Karin, M. (2006). Intracellular pattern recognition receptors in the host response. Nature *442*, 39-44.
Mibayashi, M., Martinez-Sobrido, L., Loo, Y. M., Cardenas, W. B., Gale, M., Jr., and Garcia-Sastre, A. (2007). Inhibition of retinoic acid-inducible gene I-mediated induction of beta interferon by the NS1 protein of influenza A virus. J Virol *81*, 514-524.
Michallet, M. C., Meylan, E., Ermolaeva, M. A., Vazquez, J., Rebsamen, M., Curran, J., Poeck, H., Bscheider, M., Hartmann, G., Konig, M., *et al.* (2008). TRADD protein is an essential component of the RIG-like helicase antiviral pathway. Immunity *28*, 651-661.
Oganesyan, G., Saha, S. K., Guo, B., He, J. Q., Shahangian, A., Zarnegar, B., Perry, A., and Cheng, G. (2006). Critical role of TRAF3 in the Toll-like receptor-dependent and -independent antiviral response. Nature *439*, 208-211.
O'Neill, L. A., and Bowie, A. G. (2007). The family of five: TIR-domain-containing adaptors in Toll-like receptor signalling. Nat Rev

Immunol *7*, 353-364.
Palm, N. W., and Medzhitov, R. (2009). Pattern recognition receptors and control of adaptive immunity. Immunol Rev *227*, 221-233.
Panne, D. (2008). The enhanceosome. Curr Opin Struct Biol *18*, 236-242.
Park, B., Brinkmann, M. M., Spooner, E., Lee, C. C., Kim, Y. M., and Ploegh, H. L. (2008). Proteolytic cleavage in an endolysosomal compartment is required for activation of Toll-like receptor 9. Nat Immunol *9*, 1407-1414.
Pavri, R., Zhu, B., Li, G., Trojer, P., Mandal, S., Shilatifard, A., and Reinberg, D. (2006). Histone H2B monoubiquitination functions cooperatively with FACT to regulate elongation by RNA polymerase II. Cell *125*, 703-717.
Peng, J., Schwartz, D., Elias, J. E., Thoreen, C. C., Cheng, D., Marsischky, G., Roelofs, J., Finley, D., and Gygi, S. P. (2003). A proteomics approach to understanding protein ubiquitination. Nat Biotechnol *21*, 921-926.
Perry, A. K., Chow, E. K., Goodnough, J. B., Yeh, W. C., and Cheng, G. (2004). Differential requirement for TANK-binding kinase-1 in type I interferon responses to toll-like receptor activation and viral infection. J Exp Med *199*, 1651-1658.
Pichlmair, A., Schulz, O., Tan, C. P., Naslund, T. I., Liljestrom, P., Weber, F., and Reis e Sousa, C. (2006). RIG-I-mediated antiviral responses to single-stranded RNA bearing 5'-phosphates. Science *314*, 997-1001.
Pickart, C. M. (2001). Mechanisms underlying ubiquitination. Annu Rev Biochem *70*, 503-533.
Pickart, C. M. (2004). Back to the future with ubiquitin. Cell *116*, 181-190.
Pickart, C. M., and Eddins, M. J. (2004). Ubiquitin: structures, functions, mechanisms. Biochim Biophys Acta *1695*, 55-72.
Pippig, D. A., Hellmuth, J. C., Cui, S., Kirchhofer, A., Lammens, K., Lammens, A., Schmidt, A., Rothenfusser, S., and Hopfner, K. P. (2009). The regulatory domain of the RIG-I family ATPase LGP2 senses double-stranded RNA. Nucleic Acids Res.
Plafker, S. M., Plafker, K. S., Weissman, A. M., and Macara, I. G. (2004). Ubiquitin charging of human class III ubiquitin-conjugating enzymes triggers their nuclear import. J Cell Biol *167*, 649-659.
Poltorak, A., He, X., Smirnova, I., Liu, M. Y., Van Huffel, C., Du, X., Birdwell, D., Alejos, E., Silva, M., Galanos, C., *et al.* (1998). Defective LPS signaling in C3H/HeJ and C57BL/10ScCr mice: mutations in Tlr4 gene. Science *282*, 2085-2088.

Rothenfusser, S., Goutagny, N., DiPerna, G., Gong, M., Monks, B. G., Schoenemeyer, A., Yamamoto, M., Akira, S., and Fitzgerald, K. A. (2005). The RNA helicase Lgp2 inhibits TLR-independent sensing of viral replication by retinoic acid-inducible gene-I. J Immunol *175*, 5260-5268.

Ryzhakov, G., and Randow, F. (2007). SINTBAD, a novel component of innate antiviral immunity, shares a TBK1-binding domain with NAP1 and TANK. Embo J *26*, 3180-3190.

Saha, S. K., Pietras, E. M., He, J. Q., Kang, J. R., Liu, S. Y., Oganesyan, G., Shahangian, A., Zarnegar, B., Shiba, T. L., Wang, Y., and Cheng, G. (2006). Regulation of antiviral responses by a direct and specific interaction between TRAF3 and Cardif. Embo J *25*, 3257-3263.

Sasai, M., Shingai, M., Funami, K., Yoneyama, M., Fujita, T., Matsumoto, M., and Seya, T. (2006). NAK-associated protein 1 participates in both the TLR3 and the cytoplasmic pathways in type I IFN induction. J Immunol *177*, 8676-8683.

Seth, R. B., Sun, L., Ea, C. K., and Chen, Z. J. (2005). Identification and characterization of MAVS, a mitochondrial antiviral signaling protein that activates NF-kappaB and IRF 3. Cell *122*, 669-682.

Sharma, S., tenOever, B. R., Grandvaux, N., Zhou, G. P., Lin, R., and Hiscott, J. (2003). Triggering the interferon antiviral response through an IKK-related pathway. Science *300*, 1148-1151.

Stack, J., Haga, I. R., Schroder, M., Bartlett, N. W., Maloney, G., Reading, P. C., Fitzgerald, K. A., Smith, G. L., and Bowie, A. G. (2005). Vaccinia virus protein A46R targets multiple Toll-like-interleukin-1 receptor adaptors and contributes to virulence. J Exp Med *201*, 1007-1018.

Steel, J., Lowen, A. C., Pena, L., Angel, M., Solorzano, A., Albrecht, R., Perez, D. R., Garcia-Sastre, A., and Palese, P. (2009). Live attenuated influenza viruses containing NS1 truncations as vaccine candidates against H5N1 highly pathogenic avian influenza. J Virol *83*, 1742-1753.

Stetson, D. B., and Medzhitov, R. (2006). Type I interferons in host defense. Immunity *25*, 373-381.

Stojdl, D. F., Lichty, B. D., tenOever, B. R., Paterson, J. M., Power, A. T., Knowles, S., Marius, R., Reynard, J., Poliquin, L., Atkins, H., *et al.* (2003). VSV strains with defects in their ability to shutdown innate immunity are potent systemic anti-cancer agents. Cancer Cell *4*, 263-275.

Stuart, L. M., and Ezekowitz, R. A. (2008). Phagocytosis and comparative innate immunity: learning on the fly. Nat Rev Immunol *8*, 131-141.

Summers, M. K., Pan, B., Mukhyala, K., and Jackson, P. K. (2008). The unique N terminus of the UbcH10 E2 enzyme controls the threshold for APC activation and enhances checkpoint regulation of the APC. Mol Cell *31*, 544-556.
Sun, Q., Sun, L., Liu, H. H., Chen, X., Seth, R. B., Forman, J., and Chen, Z. J. (2006). The specific and essential role of MAVS in antiviral innate immune responses. Immunity *24*, 633-642.
Takeuchi, O., and Akira, S. (2008). MDA5/RIG-I and virus recognition. Curr Opin Immunol *20*, 17-22.
Tang, E. D., and Wang, C. Y. (2009). Mavs Self-Association Mediates Antiviral Innate Immune Signaling. J Virol.
Tanner, N. K., and Linder, P. (2001). DExD/H box RNA helicases: from generic motors to specific dissociation functions. Mol Cell *8*, 251-262.
Tenno, T., Fujiwara, K., Tochio, H., Iwai, K., Morita, E. H., Hayashi, H., Murata, S., Hiroaki, H., Sato, M., Tanaka, K., and Shirakawa, M. (2004). Structural basis for distinct roles of Lys63- and Lys48-linked polyubiquitin chains. Genes Cells *9*, 865-875.
Underhill, D. M., and Ozinsky, A. (2002). Phagocytosis of microbes: complexity in action. Annu Rev Immunol *20*, 825-852.
VanDemark, A. P., Hofmann, R. M., Tsui, C., Pickart, C. M., and Wolberger, C. (2001). Molecular insights into polyubiquitin chain assembly: crystal structure of the Mms2/Ubc13 heterodimer. Cell *105*, 711-720.
Varadan, R., Assfalg, M., Haririnia, A., Raasi, S., Pickart, C., and Fushman, D. (2004). Solution conformation of Lys63-linked di-ubiquitin chain provides clues to functional diversity of polyubiquitin signaling. J Biol Chem *279*, 7055-7063.
Venkataraman, T., Valdes, M., Elsby, R., Kakuta, S., Caceres, G., Saijo, S., Iwakura, Y., and Barber, G. N. (2007). Loss of DExD/H box RNA helicase LGP2 manifests disparate antiviral responses. J Immunol *178*, 6444-6455.
Vilcek, J. (2006). Fifty years of interferon research: aiming at a moving target. Immunity *25*, 343-348.
Williams, B. R. (2001). Signal integration via PKR. Sci STKE *2001*, RE2.
Williams, M. J. (2007). Drosophila hemopoiesis and cellular immunity. J Immunol *178*, 4711-4716.
Wu, C. J., Conze, D. B., Li, T., Srinivasula, S. M., and Ashwell, J. D. (2006). Sensing of Lys 63-linked polyubiquitination by NEMO is a key event in NF-kappaB activation [corrected]. Nat Cell Biol *8*, 398-406.

Xiang, Y., Condit, R. C., Vijaysri, S., Jacobs, B., Williams, B. R., and Silverman, R. H. (2002). Blockade of interferon induction and action by the E3L double-stranded RNA binding proteins of vaccinia virus. J Virol *76*, 5251-5259.

Xu, L. G., Wang, Y. Y., Han, K. J., Li, L. Y., Zhai, Z., and Shu, H. B. (2005). VISA is an adapter protein required for virus-triggered IFN-beta signaling. Mol Cell *19*, 727-740.

Yoneyama, M., Kikuchi, M., Matsumoto, K., Imaizumi, T., Miyagishi, M., Taira, K., Foy, E., Loo, Y. M., Gale, M., Jr., Akira, S., *et al.* (2005). Shared and unique functions of the DExD/H-box helicases RIG-I, MDA5, and LGP2 in antiviral innate immunity. J Immunol *175*, 2851-2858.

Yoneyama, M., Kikuchi, M., Natsukawa, T., Shinobu, N., Imaizumi, T., Miyagishi, M., Taira, K., Akira, S., and Fujita, T. (2004). The RNA helicase RIG-I has an essential function in double-stranded RNA-induced innate antiviral responses. Nat Immunol *5*, 730-737.

Zhang, M., Wu, X., Lee, A. J., Jin, W., Chang, M., Wright, A., Imaizumi, T., and Sun, S. C. (2008). Regulation of IkappaB kinase-related kinases and antiviral responses by tumor suppressor CYLD. J Biol Chem *283*, 18621-18626.

Zhang, P., and Samuel, C. E. (2008). Induction of protein kinase PKR-dependent activation of interferon regulatory factor 3 by vaccinia virus occurs through adapter IPS-1 signaling. J Biol Chem *283*, 34580-34587.

Zhao, T., Yang, L., Sun, Q., Arguello, M., Ballard, D. W., Hiscott, J., and Lin, R. (2007). The NEMO adaptor bridges the nuclear factor-kappaB and interferon regulatory factor signaling pathways. Nat Immunol *8*, 592-600.

Zhong, B., Yang, Y., Li, S., Wang, Y. Y., Li, Y., Diao, F., Lei, C., He, X., Zhang, L., Tien, P., and Shu, H. B. (2008). The adaptor protein MITA links virus-sensing receptors to IRF3 transcription factor activation. Immunity *29*, 538-550.